SKB

TECHNICAL REPORT 91-58

Exploratory calculations concerning the influence of glaciation and permafrost on the groundwater flow system, and an initial study of permafrost influences at the Finnsjön site – an SKB 91 study

Björn Lindbom, Anders Boghammar

Kemakta Konsult AB, Stockholm

December 1991

SVENSK KÄRNBRÄNSLEHANTERING AB
SWEDISH NUCLEAR FUEL AND WASTE MANAGEMENT CO

BOX 5864 S-102 48 STOCKHOLM

TEL 08-665 28 00 TELEX 13108 SKB S
TELEFAX 08-661 57 19

EXPLORATORY CALCULATIONS CONCERNING THE INFLUENCE OF GLACIATION AND PERMAFROST ON THE GROUNDWATER FLOW SYSTEM, AND AN INITIAL STUDY OF PERMAFROST INFLUENCES AT THE FINNSJÖN SITE - AN SKB 91 STUDY

Björn Lindbom, Anders Boghammar

Kemakta Konsult AB, Stockholm

December 1991

Exploratory calculations concerning the influence of glaciation and permafrost on the groundwater flow system, and an initial study of permafrost influences at the Finnsjön site – an SKB 91 study

by

Björn Lindbom
Anders Boghammar

Kemakta Konsult AB
Pipersgatan 27
112 28 Stockholm

Abstract

The present report describes some exploratory calculations concerning the potential groundwater flow during the recession phase of a future glaciation. The exercise forms part of the SKB 91 performance assessment project, and aims at qualitatively illustrating the prevailing hydrological phenomena under extreme glacier conditions, and at quantitatively indicating the order of magnitudes for the groundwater flows that can be expected during the withdrawal of an ice-sheet. The interest has been focussed on the deglaciation phase, since it can be expected that large amounts of water are available for infiltration at this time. Conditions assuming either intact or melted away permafrost were considered within the project.

Apart from the exploratory calculations mentioned above, an initial attempt at modelling a permafrost situation at the Finnsjön site was carried out. This part of the study did not include the presence of melting-water, but was focussed on the potential occurrence of permafrost and its impact on the groundwater flow as a potential barrier. These calculations are reported separately in an Appendix.

Neither part of the project addressed the conceptual uncertainties like potential crustal downwarping, thermal buoyancy effects by the heat evolution from the repository, fracture zone conductivities being affected by the overburden from the ice-shelf, etc, etc.

The project made use of the finite element code NAMMU for solving the equation system, while the program package HYPAC was used for pre- and postprocessing purposes.

Summary

The present exercise forms part of the SKB 91 performance assessment project, and is concerned with exploratory numerical calculations of the groundwater flow during the recession phase of a glaciation. The modelling was generic in two dimensions, and was oriented towards the expected high flow conditions that can be assumed during a deglaciation phase. Situations either without permafrost or a 100 m thick layer of permafrost were assumed. Two cases were studied with scenarios differing mainly with regard to the specified boundary condition along the top boundary. The main cases were concerned with a pressure boundary condition with the shape, or pressure distribution, corresponding to that of an ice-sheet. Hydraulic conductivities were representative of the Finnsjö-site, which has been subjected to extensive field investigations.

The main conclusions that were drawn from the study could be collected accordingly:

Large amounts of water penetrate into the (surficial) part of the bedrock. The major part (90 %) was discharged horizontally at the very ice-front, while the remaining part was infiltrated vertically into the bedrock. The latter was subject to an extreme peak behaviour just by the ice-front. For the main part of the studied cases, roughly 90 % of the melting water was recharged during the final 10 kilometres of the total infiltration area which was 110 kilometres long. The melting water for the main cases amounted to about 800 m^3/year, where roughly 90 % was discharged horizontally at the ice-front. The extreme peak behaviour was observed both on the recharge side and the discharge side in the very proximity of the ice-front. The peak behaviour took place for a distance of about 70-80 kilometres.

The flux peak values at repository level were roughly $4 \cdot 10^{-3}$ m^3/m^2/year, and with an assumption of a porosity equal to 10^{-4}, the travel times for particles released at repository level were in the range 100-1000 years, corresponding to an uncertainty of 10-100 km in space if a glacier withdrawal of 100 m/year is assumed.

When permafrost conditions were assumed, a local retarding influence from it was observed. The influence in time was restricted to be in the same order as the occurrence of the peak values of the melting water as discussed above. The retarding effect would surely have been more pronounced, had a thicker layer of permafrost been assumed. However, a limited duration would probably have been the situation also for this case.

Despite the conceptual uncertainties and lack of data, a reasonable degree of confidence could be put into the results. This statement is based on the results from the calculation of total flow along the top boundary, which appeared to be in amazingly good agreement with the values that initially were discussed as the geothermal melting capacity. The latter is assumed to be about 50 mm/year, corresponding to an inflow over the region of 750 m^3/year, to be compared with the calculated value of 800 m^3/year for the main cases. Of course, the calculated flow is a function of the hydraulic conductivities assigned to the bedrock, so the good match between estimated melting capacity and the calculated amount of melting water could be regarded as a good "guesstimate" when the hydraulic properties were assigned. Nevertheless, the results seem to indicate values that at least are in the right order of magnitude under the circumstances, and by this one can state that the approach taken seems to hold, at least serving as a basis for future studies in the area of glaciations and the extreme flow conditions that prevail during the de-glaciation phase.

Despite that the project has shed light on some interesting phenomena related to the performance of a potential repository during a de-glaciation phase, there are some conceptual uncertainties that should be mentioned. These could for instance be the hydraulic conductivity of the host rock when being severely compressed by the ice-burden, internal fracturing in the ice-sheet due to run-off of melting water and high pressures, the closing or widening-up of fracture zones being subject to high pressures from partly the ice-sheet itself and partly by the pressure from the melting water, the porosity of the host rock when being compressed, which affects the travel times for particles escaping from the repository, the effect from the potential crustal downwarping, etc, etc. Since the

present project was intended to be exploratory, it was beyond its scope to analyse the model sensitivity to the conceptual uncertainties mentioned above. It is therefore recommended that future studies should be focussed on these issues.

An initial attempt at modelling the different stages of the permafrost evolution prior to a glaciation addressed the risk of a maintained heat evolution from the potential repository, which may degrade the permafrost barrier. The study was concerned with the Finnsjön site, and it was shown that the permafrost well may act as an effective barrier, but this was conditioned by the depth of the permafrost relative to the depth of zone 2. When the upper parts of the domain consisted of permafrost, no effect at all was seen with regard to the fluxes at repository level. However, when the permafrost penetrated down to the lower confinement of zone 2, an increase in flow by a factor of 8 was observed; from the natural flow of $5 \cdot 10^{-6}$ $m^3/m^2/year$ to about $4 \cdot 10^{-5}$ $m^3/m^2/year$.

The particle tracking showed further evidence for the vertical separation of the flow domain caused by zone 2 and its interaction with the bounding fracture zones. The case with permafrost above zone 2 showed that the particles, regardless of release position, were discharged in the bounding zone 1 via zone 2. The situation with permafrost down to the lower confinement of zone 2 showed that the particles in this case were discharged through the bedrock to zone 1. This case showed travel times (porosity = 10^{-4}) of around $2 \cdot 10^3$ years from the repository.

Table of Contents

1. Introduction

The present study forms part of the SKB 91 performance assessment project. The study aims at giving a broad overview of the potential groundwater flow in the melting-away phase of a glacier, by means of numerical modelling. The interest has been raised since it can be assumed that the amounts of melting water in the deglaciation phase can be rather substantial, and by this possibly affect the performance of a potential repository for spent nuclear fuel. The presence of permafrost in the vicinity of the ice-front could also affect the function of the repository, by means of either retarding the release processes due to the stagnant (frozen) water, or by means of an increased flow through the repository if the permafrost is assumed to be melted. The latter issue has been addressed by means of a site-specific modelling of the Finnsjön site, where the pre-glacial phase has been studied, with particular interest on different stages of melted away permafrost. These modelling results are reported in Appendix A in this report.

1.1 Aims of the Project

The ultimate aim of the study is to give an overview of the groundwater flow in the area of the potential repository during the melting phase of a glaciation taking place 10000-30000 years from now with an expected maximum around 20000 years from now. The present project has to be regarded as an introductory study, which means that the results from the project hopefully could elucidate some aspects that could be recommended for future work in the area, rather than forecasting actual future conditions. This restriction is mainly due to lack of input data, but also to rather large conceptual uncertainties. The latter comprise for instance conductivity of the bedrock with high overburden pressures from the ice-sheet, fracturing, infiltration capacity, etc. Only purely fresh-water, iso-thermal and steady-state conditions are assumed.

The calculations performed within the study are based on the finite element method and involved the use of the NAMMU-code (Rae J, et al, 1979, and Atkinson R, et al, 1985) for solving the equation system, while the program package HYPAC (Grundfelt B, et al, 1989) was used for pre- and postprocessing purposes.

1.2 Scope of the Project

The primary intention is to describe the geohydrological conditions during the withdrawal of an ice-sheet from the repository area. The modelling is carried out in a generic manner.

The domain is modelled in two dimensions. A pre-study has been carried out on the scale of about 100 km, with the aim of reducing the domain to be on the scale of some tens of kilometres by transferring the pressure boundary conditions from the pre-study cases to the main generic cases. The latter being on the scale of about 30 km. Although fracture zones are assumed to exist, they are omitted due to the scaling problem, the rock mass is rather regarded as a porous medium with inherent fracture zone properties. Four cases are studied with different combinations of permafrost and pressure boundary conditions along the top boundary.

As mentioned above, an initial study with regard to the influences on the groundwater flow at the Finnsjön site that can be expected from permafrost conditions during the pre-glacial phase, is presented in Appendix A.

2. Scenario Description

According to (Ahlbom K, et al, 1991) it is likely that northern Europe will be subjected to glaciations with a certain periodicity. Climatic conditions similar to those of today are anticipated to prevail at a time of about 120000 years from now. In the mean time, three glaciations are likely to occur:

- The first with a maximum at 5000 years A.P. (After Present) with an ice-sheet covering the scandinavian mountainous region.
- The second with a maximum at 20000 years A.P. with an ice-sheet covering Norway, Finland, and the northern part of Sweden with the south-most third un-covered by ice.
- The third with a maximum at 60000 years with an ice-sheet covering Norway, Sweden, Finland, the Baltic states, some 1000 kilometres of the eastern part of Soviet Union, and the northern part of Germany.

The first glaciation is deemed to be of minor importance from the point of view of safety of a radioactive waste repository, since it covers areas that probably are located far away from potential disposal sites. This report is concerned with the second glaciation.

The general understanding is that a glaciation is preceded by tundra-like conditions followed by permafrost. During the glaciation, it is assumed that one part of the bedrock is constituted by permafrost, and one part with areas beneath the ice-sheet with no permafrost but with rather large amounts of melting water at the interface between the ice and the bedrock. The most interesting scenario to study in this context, is the deglaciation phase, i.e. when large amounts of melting water are accessible for infiltration into the bedrock with a simultaneous permafrost recession. The hydraulic driving force at this time is the water from beneath the ice-sheet, which has been melted away mainly due to the heat from the earth, and to a minor degree due to the warming up of the atmosphere. At this point in time of the deglaciation, permafrost is assumed to be partly recessed so that it occurs to a certain extent to a certain depth beyond the ice-front. The part of the bedrock that is located below the ice-sheet is assumed to be warmed up during the deglaciation, so that no permafrost is present here.

3. Conceptualisation of the Scenario

The geometry of the domain is schematically shown in Figure 3.1, intentionally without scales or dimensions. The vertical extent of the permafrost is uncertain. According to conditions in Great Britain during the glaciations for the last 750000 years, the permafrost penetrated down to about 250 m at its most (Boulton G, 1991). Considering that the geothermal gradient in Scandinavia is about half that of Great Britain, a reasonable value could be about 500 m depth as a maximum for the permafrost to penetrate for the current study. However, since the intention is to study the deglaciation phase, one could surely assume that the depth of the permafrost is considerably less than so. Thus, the assumption for the present study is that the permafrost is located down to a depth of 100 m from the ground surface.

The topography over the entire domain is flat, i.e. the only driving force for the groundwater flow is the pressure gradient induced by the overburden caused by the ice-sheet and the melting water that is assumed to infiltrate from the ice into the bedrock. The geometry of the ice-sheet is based on an expression theoretically derived by (Embleton C, and King C A M, 1975) obeying the formula $H=4.76\sqrt{R}$, where H is the thickness of the ice-sheet and R is the horizontal extent of the ice-sheet. This expression was found to fit measured values in the Antarctic with rather good agreement with certain simplifications with regard to temperature distribution and shear stress etc. This curve is plotted in Figure 3.2.

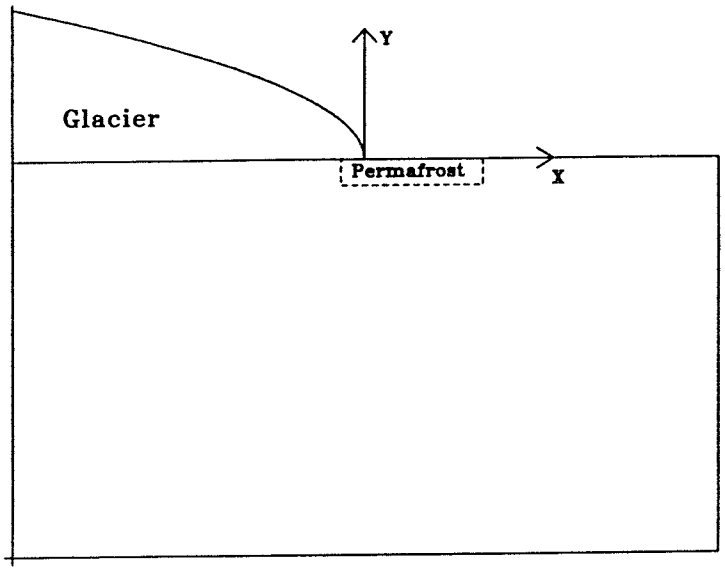

Figure 3.1 *Schematic of the domain to be studied.*

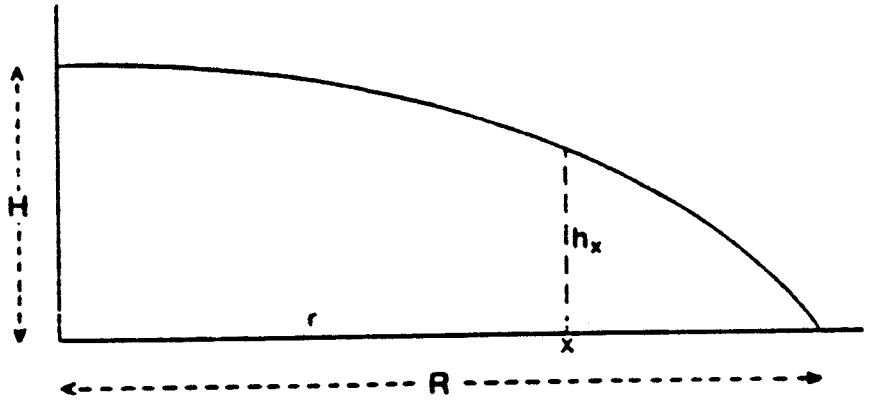

Figure 3.2 *Cross section through a glacier as considered for the present study. The curve $H=4.76\sqrt{R}$ describes the thickness (H) of the ice-sheet as a function of the horizontal extent (R) as calculated by (Embleton C, and King C A M, 1975).*

The maximum thickness of the ice-sheet is assumed to be 1500 m and its horizontal extent is shown in Figure 3.3. The distance from the centre of the glacier to the ice-front is roughly 1000 kilometres in a southward direction, where it reaches the area north of Stockholm. At this position, the horizontal extent of the permafrost is assumed to coincide with the ice-front. If going a direction to the south-most part of Sweden from the core of the ice-sheet, the horizontal extent of the permafrost beyond the ice-front is about 500 km.

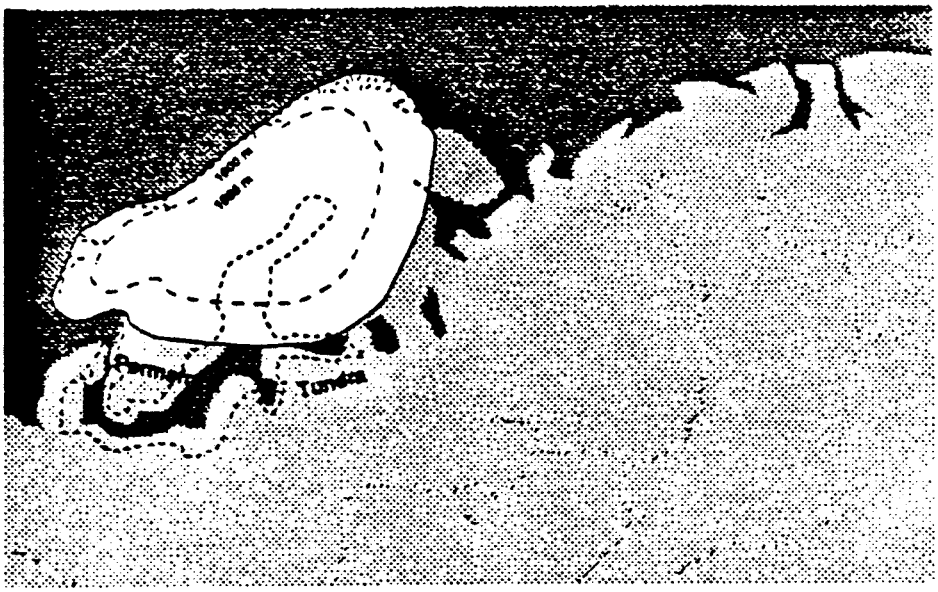

Figure 3.3 *Evolution of the ice-sheet of a glaciation taking place about 10000-30000 years from now, with an expected maximum at about 20000 years from now (Ahlbom K, et al, 1991).*

One source of uncertainty is the extent of the permafrost layer in the melting phase, since the modelling results largely could depend on the position of the permafrost relative to the position of the outlet boundary. This concern is based on that large amounts of water are imposed along the glacier-bedrock interface to the left in Figure 3.1. This water has to be discharged through the domain, which in turn means that the position of the outlet boundary is important in order to avoid geometry-dependent results – particularly if an impermeably layer (i.e. the permafrost) is considered for part of the outlet domain. One could assume that the permafrost takes a certain time to develop, a time that depends on the prevailing climatic conditions. According to (Boulton G, 1991), it takes about 50 years to develop a permafrost layer with 100 m thickness assuming a cooling of the surface with 1° K/year. Assuming that the recession of the permafrost is of about the same rate, it would imply that a permafrost layer of 100 m thickness is completely melted away at one end, and still 100 m thick at the other end, i.e. the one coinciding with the ice-front in Figure 3.1. However, for simplifying reasons, a rectangular shape of the permafrost layer has been assumed. The lateral extent of the permafrost thus amounts to 5000 m (100 m/year·50 years). Furthermore, the permafrost has been assumed to extend laterally 1 km beneath the ice-sheet.

The hydraulic conductivity of the bedrock (the K-value) is assumed to be identical to the value used for previous modelling exercises at the Finnsjön site. One could argue that the bedrock is intact at the time of a glaciation. Due to the heavy overburden from the ice-sheet, the bedrock is surely compressed and fracture zone planes are likely to be linked more closely due to this, if not sheared. On the other hand, vertical or subvertical fracture zones will be subjected to extremely high pressure from the ice-sheet or from the melted water beneath the ice-sheet, which implies that the fracture zone planes may be subject to

detaching movements, thus increasing their transmissivities. Due to these contradictory conceptual uncertainties, it was decided that the bedrock conductivity would be maintained according to the Finnsjö-data as reported by (Andersson J-E, et al, 1991), and let these uncertainties serve as a basis for sensitivity analysis.

Fracture zones, both regional lineaments and local zones, vertical as well as horizontal are likely to occur wherever in the bedrock. Either type could be assumed to occur with a certain frequency and with certain water-bearing capacities, and consequently they should be included in the calculations. However, the scale of concern is some tens of kilometres to hundreds of kilometres, which ought to be compared to the scale of the fracture zones (tens or in some instances hundreds of metres), which makes an incorporation of the fracture zones meaningless. On the whole, they would not be visible when using the porous media approach, at least not with the conductivity contrasts that are at hand. Therefore, the bedrock is regarded as a porous medium into which the fracture zone properties are averaged, thus fracture zones are discarded from a modelling point of view. Furthermore, fracture zones were omitted for the sake of consistency with the discussion in the previous paragraph.

The boundary conditions of concern may be either of Neuman-type, i.e. a prescribed flow rate, or of Dirichlet-type, i.e. a prescribed pressure. The former could be based on the assumption that a certain amount of water is melted away beneath the ice-sheet, and accordingly free to infiltrate through the top surface of the bedrock. The amount of melting water per volume unit of the area beneath the ice-sheet could be determined on the basis of the geothermal melting capacity; values of around 50 mm/year have been discussed in this context. However, there are large uncertainties with regard to the amount of water that infiltrates and contributes to the groundwater formation, and corresponding amounts that are discharged at the ice-front or in fractures or tunnel-like formations within the ice-sheet. Furthermore, there seems to be a consensus that permafrost is likely to occur discontinuously not only beyond the ice-front, but also in the ground that is covered by ice. This would imply that there is another source of uncertainty at hand with regard to the amount of water that is assumed to penetrate into the bedrock, since the presence of permafrost effectively will prevent water from both infiltration and by-pass transport to the ice-front for a discharge. Due to the large conceptual uncertainties with regard to the amount of water that infiltrates through the bedrock, this type of boundary condition is discarded. The second type of boundary condition assumes that the overburden of the ice-sheet imposes a pressure on the melting water, i.e. in a sense forces the water to penetrate through the top layer of the bedrock. There have been discussions on how large the applied pressure could be. According to observations and measurements in the Antarctic, there is reason to believe that pressures far higher than 4000 kPa may be present beneath the ice-sheet, in fact there are observations that support the idea of imposing a pressure boundary that corresponds to the entire thickness of the ice-sheet. Therefore, this approach is chosen within the present study, which means that the applied pressure along the top boundary amounts to 15000 kPa at its maximum, which corresponds to a maximum thickness of the ice-sheet of 1500 m.

The approach with a water pressure corresponding to the elevation of the ice-sheet, is also supported in (Rosengren and Stephanson, 1990), where rock mass responses to glaciations were modelled and analysed. In one of the cases in the cited study, an ice-lake was assumed to appear in the deglaciation phase, thus imposing a pore water pressure equal to the hydrostatic pressure in the bedrock for the part of the domain that was located below the ice-lake. The part of the domain that was still covered by ice was modelled with a pore water pressure corresponding to the elevation of the ice-sheet. However, it should be mentioned that the cited study was not intended to describe the groundwater flow, but was oriented towards rock mechanics.

4. Case Descriptions and Nomenclature

4.1 Modelling Approach

In order to account for the complete areal coverage of the ice-sheet in the numerical model, the lateral extent of the model should be about 1000 km from the core of the glacier to the ice-front. Since the geometrical scale of a model with such dimensions is difficult to handle and to visualise, and also untractable for numerical reasons, it is desireable to reduce the domain to be modelled. Furthermore, since the position of the lateral boundary on the part of the domain that is free of ice surely affects the modelling results, the lateral extent of the model beyond the ice-front is somewhat uncertain. In order to elucidate the effects from the position of the lateral boundaries relative to the extreme boundary conditions that are imposed, a pre-study was considered necessary to establish a reasonable geometry of the modelled domain in order both to avoid geometry-dependent results, and to have the domain reduced. The pre-study cases consider a horizontal extent of the glacier to 110 km upstream the ice-front, a length at which the height of the glacier is fully evolved, 1500 m. The area farther away than 110 km upstream the ice-front is not considered; this area is rather looked upon as a flat region with no topography. The pre-study cases, or "full scale" models are regarded as tools in order to penetrate into the main cases that are reduced in size, and are modelled merely in order to transfer lateral boundary pressures to the "reduced-size" cases. This procedure is dealt with in Appendix B, and the following sections are entirely concerned with cases extending only 15 km on each side of the ice-front, whereas the full scale model extend 110 km on each side of the ice-front.

A full description of the pre-study is given in Appendix B.

4.2 Input Data

Four cases are included in the study. As indicated earlier, the host rock is assumed to be homogeneous and isotropic with a depth dependent hydraulic conductivity. The cases differ only in terms of the presence of permafrost and the magnitude of the prescribed pressure along the top boundary.

Case 1 — No permafrost is assumed; pressure boundary condition under the ice-sheet corresponds to the shape of the ice-sheet. Hydraulic conductivity of the host rock corresponds to the one used in the previous Finnsjö-studies within the SKB-91 programme, i.e. $1.0 \cdot 10^{-6} \cdot z^{-1.1}$ m/s.

Case 1P — Permafrost is assumed to penetrate to a depth of 100 m, extending 5 km beyond the ice-front and 1 km beneath the ice-sheet. Hydraulic conductivity of the host rock is $1.0 \cdot 10^{-6} \cdot z^{-1.1}$ m/s.

Case 2 — The pressure boundary condition applied at the top surface is assumed to be evenly (rectangularly) distributed. The pressure corresponds to the integrated pressure in Case 1, and amounts to a level corresponding to 1000 m thick ice-sheet. Hydraulic conductivity of the host rock is $1.0 \cdot 10^{-6} \cdot z^{-1.1}$ m/s.

Case 2P — The pressure boundary condition applied at the top surface is assumed to be evenly (rectangularly) distributed. The pressure corresponds to the integrated pressure in Case 1, and amounts to a level corresponding to 1000 m thick ice-sheet. Permafrost is assumed to penetrate to a depth of 100 m, extending 5 km beyond the ice-front and 1 km beneath the ice-sheet. Hydraulic conductivity of the host rock is $1.0 \cdot 10^{-6} \cdot z^{-1.1}$ m/s.

The hydraulic conductivity of the permafrost is assumed to be 0 m/s (this value is set to 10^{-16} m/s in order to avoid numerical instabilities in NAMMU). The topography is assumed to be flat, i.e. the only driving force for the fluid is the pressure gradient induced by the overburden of the ice. The bottom boundary is located at 5 km depth and is regarded as a no-flow boundary.

The geometry of the four cases is schematically shown in Figure 3.1. The horizontal extent of the models is 30 km, 15 km on each side of the ice-front. A distance of 15 km upstream the ice-front corresponds to a position where the ice-sheet is roughly 580 m thick. The domain is discretised with about 9600 eight-noded quadri-lateral finite elements, corresponding to roughly 27000 nodal points.

5. Modelling Results

5.1 Introduction

The following chapter contains the modelling results for the four cases that were studied. The evaluation comprises particle tracking and flux distribution, and a brief analysis was also conducted for Cases 1 and 1P with regard to the infiltrated flux over the top surface of the domain, i.e. the glacier-bedrock interface.

5.2 Case 1 and Case 1P

5.2.1 Particle Tracking

Figures 5.1 (without permafrost) and 5.2 (with permafrost) show the flow paths as generated for a few particles released at the level of the potential repository. Particles 7 and 8 were released below the edge of the permafrost layer, while the remainder of the particles were released in order to see to what degree the permafrost would affect their travel paths in the vicinity of the permafrost on the upstream side. Particles 7 and 8 indicate that the influence from the permafrost on the downstream side seems to be local, since none of these particles appear to be affected to a measurable limit by the permafrost when comparing Figure 5.1 with Figure 5.2. Pathlines 2-6 act approximately as one could expect, with a rather sharp bend around the permafrost when present. Pathline 1 seems to be in accordance with particles 2-6 for Case 1 without permafrost, while it in Case 1P with permafrost is clearly affected by the permafrost. To start with it is directed downwards, but is soon being directed upwards with a weak tendency to be discharged at the ice-front. However, since the permafrost layer continues 1 km under the ice-sheet (from the ice-front), particle 1 is "trapped" and seeks its way out to be discharged among the majority of the other particles.

The travel times to the surface for a swarm of particles being released along a horizontal line at 500 m depth have been plotted as a function of their position in the domain. This is shown in Figure 5.3. A porosity of $1.0 \cdot 10^{-4}$ has been assumed when the travel times were calculated. As can be seen, the travel times are by far shorter in the neighbourhood of the ice-front for Case 1. The delaying function of the permafrost for Case 1P is most pronounced in the same area, with a difference in travel time of about 1.5 order of magnitude at its most. The retarding effect of the permafrost is located at the approximate position below the permafrost with a duration of about 5 km. What may be interesting to notice, is that the permafrost implies that the travel times are somewhat shorter also at distances way beyond the position of the permafrost layer. However, the travel times are only about half an order of magnitude shorter than in Case 1 without permafrost. Assuming a porosity of 10^{-4}, the travel times would be in the range 100-1000 years.

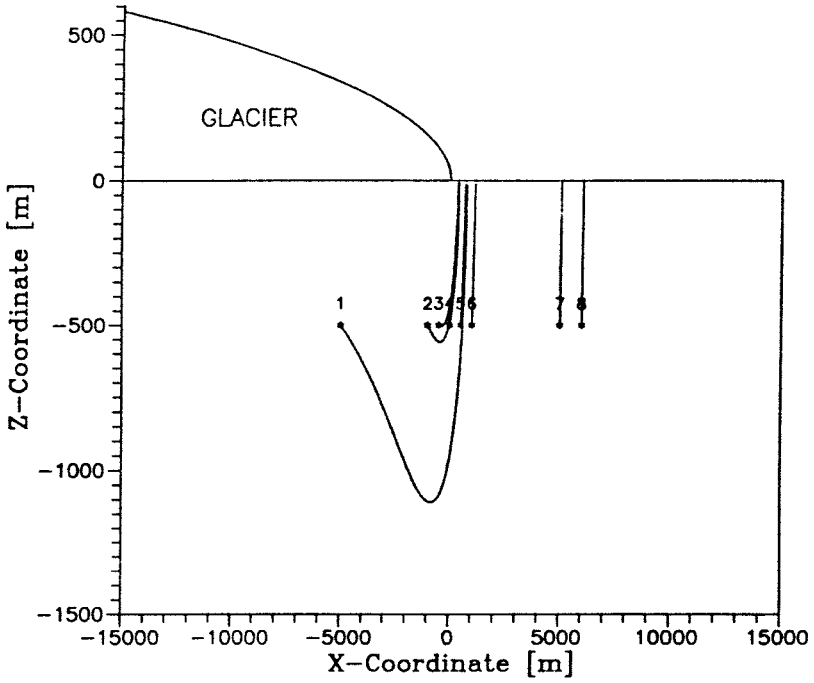

Figure 5.1 Particle tracks as generated for Case 1 (no permafrost).

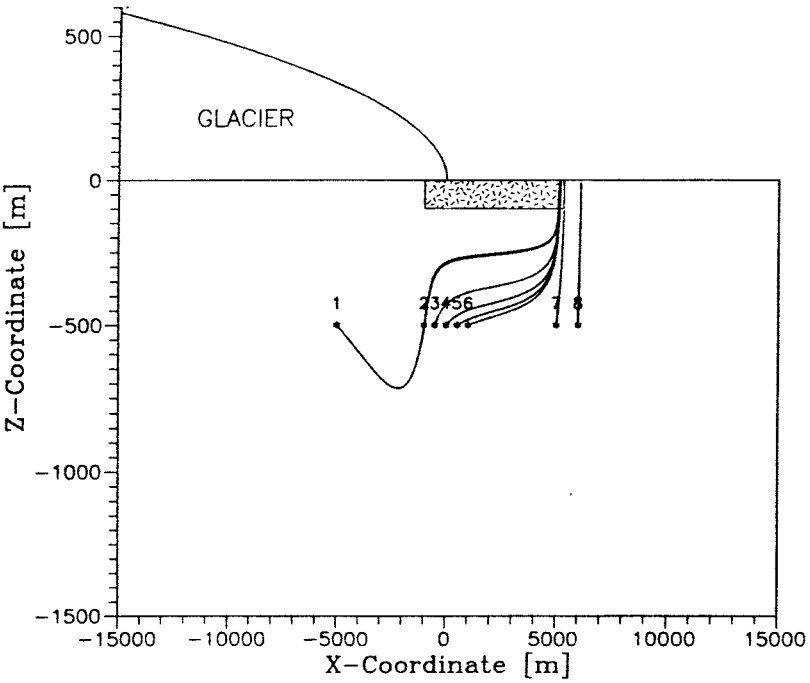

Figure 5.2 Particle tracks as generated for Case 1P (permafrost).

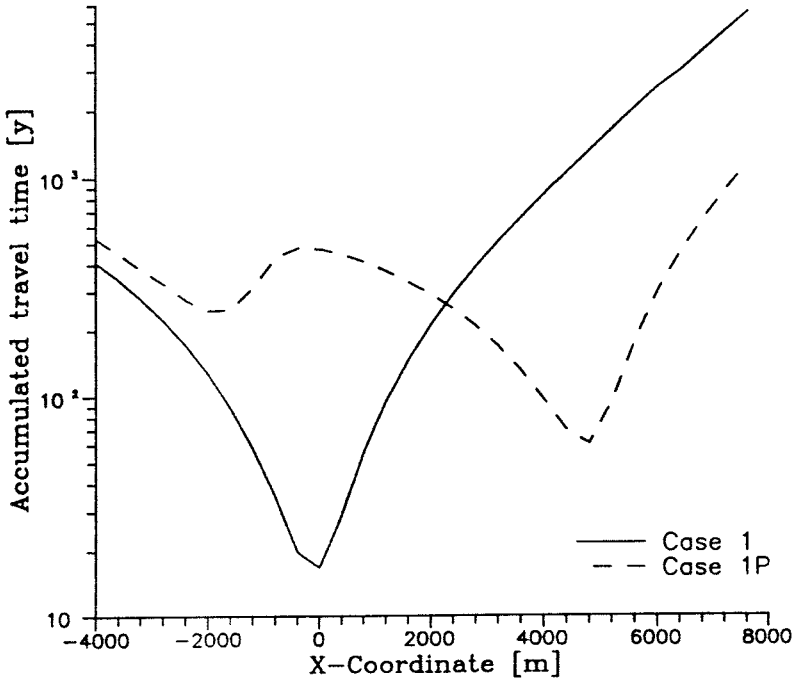

Figure 5.3 *Travel times for particles released along a horizontal line at 500 m depth for Case 1 and Case 1P. A porosity of $1.0 \cdot 10^{-4}$ has been assumed.*

5.2.2 Flux Distribution

One may notice for particle 1, that it travels deeper in Case 1 than in Case 1P, which intuitively ought to be the opposite. A brief analysis was required in order to explain this behaviour. It is caused by the peak behaviour of the system with a rather gentle vertical inflow from the ice-sheet for the major part of the domain on the inlet side. But, once being in the neighbourhood of the ice-front, the amount of water being infiltrated into the domain increases dramatically. This is shown in Figure 5.4 showing the total flux along the top boundary for the reduced domain without permafrost. (One may notice that the peak values are higher than those shown in Figure B3 in Appendix B. This effect depends on the difference in grid resolution for the calculations on the different scales; an even finer discretisation for the reduced scale may indicate even higher values than those in Figure 5.4.) When studying the vertical inflow into the domain for the situation without permafrost (Case 1) and correspondingly for the situation with permafrost (Case 1P) as shown in Figures 5.5 and 5.6, respectively, it is evident that the part of the permafrost that is located just under the ice-front reduces the amount of water that infiltrates into the domain, which explains the more shallow travel for Case 1P than in Case 1. The final kilometre of the ice-sheet just before the ice-front, is the major driving force over the domain with a gradient of about 10 %. This part of the boundary pressure was withdrawn when permafrost was assumed for Case 1P.

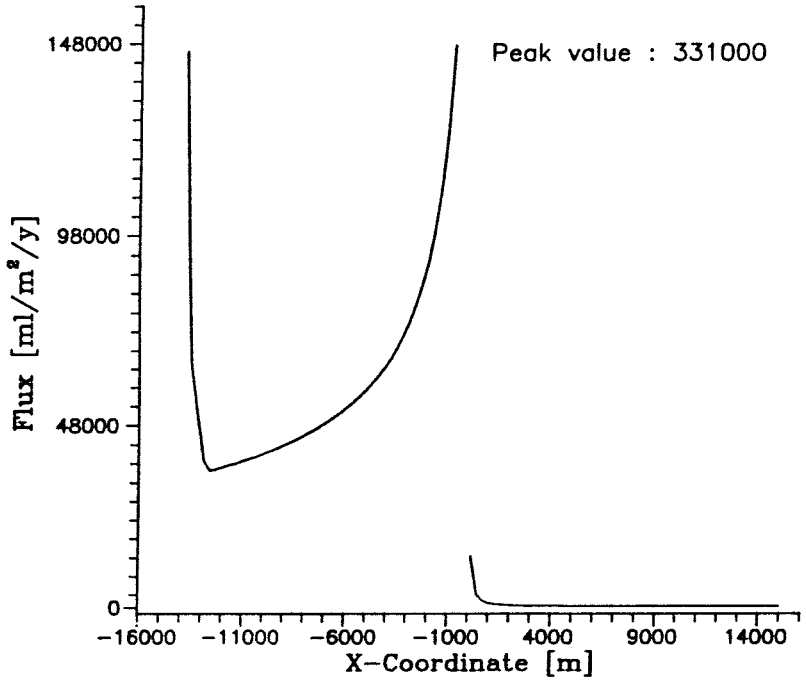

Figure 5.4 Total flux along the top boundary for Case 1 (no permafrost).

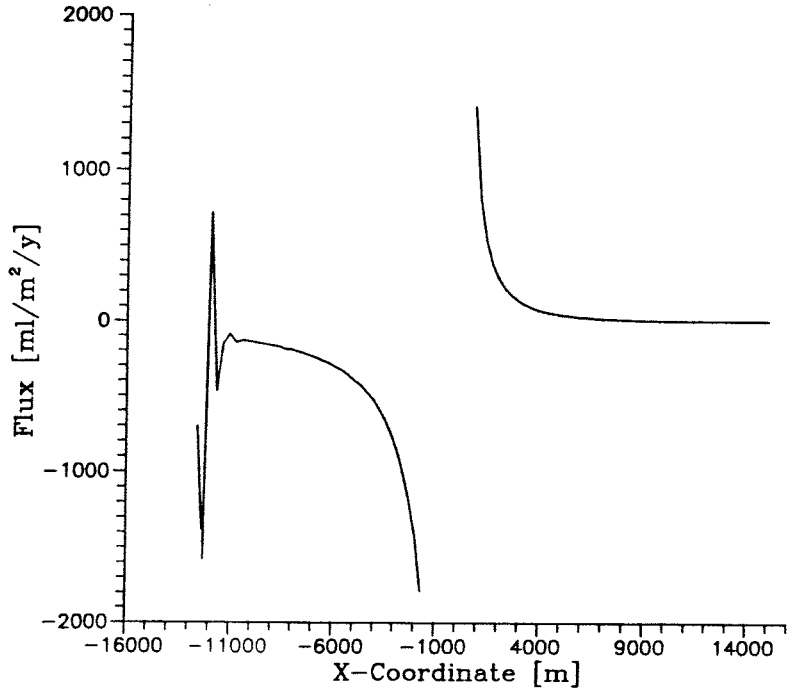

Figure 5.5 Vertical component of flux along the top boundary for Case 1 (no permafrost).

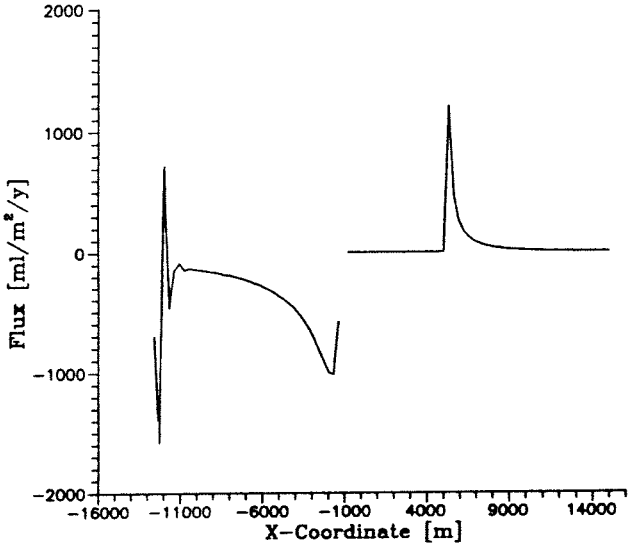

Figure 5.6 Vertical component of flux along the top boundary for Case 1P (permafrost).

Figure 5.7 shows the flux distribution along a horizontal line at 500 m depth for Case 1 and Case 1P. The peak behaviour is still visible for both cases, albeit to a lower degree than the fluxes along the top boundary. The influence from the permafrost in Case 1P is still local, it is restricted to have an impact on the results only on the scale of a few kilometres on both sides of the permafrost extension. (The influence is likely to be more pronounced along a line at a more shallow depth, since the peak behaviour is more pronounced at shallow depths, but also due to local scale phenomena in the vicinity of the permafrost.) The peak value for Case 1 is roughly $4.0 \cdot 10^{-3}$ $m^3/m^2/year$, while corresponding value for Case 1P is about $1.8 \cdot 10^{-3}$ $m^3/m^2/year$. However, due to the permafrost in Case 1P, higher flow rates than in Case 1 are observed at a distance of 1 km beyond the ice-front with values of around $0.8 \cdot 10^{-3}$ $m^3/m^2/year$ for about 4-5 km.

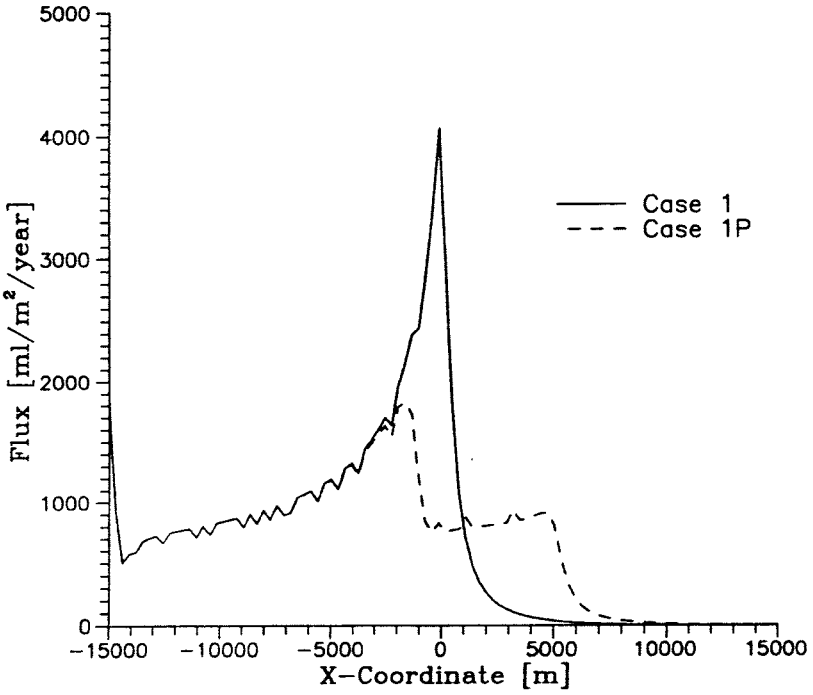

Figure 5.7 Flux values (ml/m²/year) along a line at 500 m depth for Case 1 and Case 1P.

5.2.3 Infiltration Through the Top Boundary

During the initial phase of this study, the type of top boundary condition was discussed. It could either be of a prescribed pressure type or of a prescribed infiltration type. In order to qualitatively determine the degree of confidence in model results, an analysis was made with respect to the amount of infiltrating water. Figure 5.8 shows the accumulated total flux integrated over the top part of the inlet area of the domain for Case 1 and Case 1P. From the figure, one can read out that the total flow on the top of the model is about 800 m^3/year for Case 1 and roughly 600 m^3/year for Case 1P. The lower value is an evidence for the presence of the permafrost in Case 1P, which can be seen as a flattening out of the curve in Figure 5.8 (lower).

According to the previous discussions, the geothermal melting capacity has been estimated to about 50 mm/year, which corresponds to 0.05 m^3/m^2/year over an area (1 m thick) for the cases studied of 15 km·50000 ml/year=750 m^3/year. These values are, to say the least, in amazingly good agreement with the calculated ones. However, one must bear in mind that the calculated flow is a direct function of the hydraulic conductivity of the bedrock. Nevertheless, it is comforting to see that the orders of magnitude are reasonable.

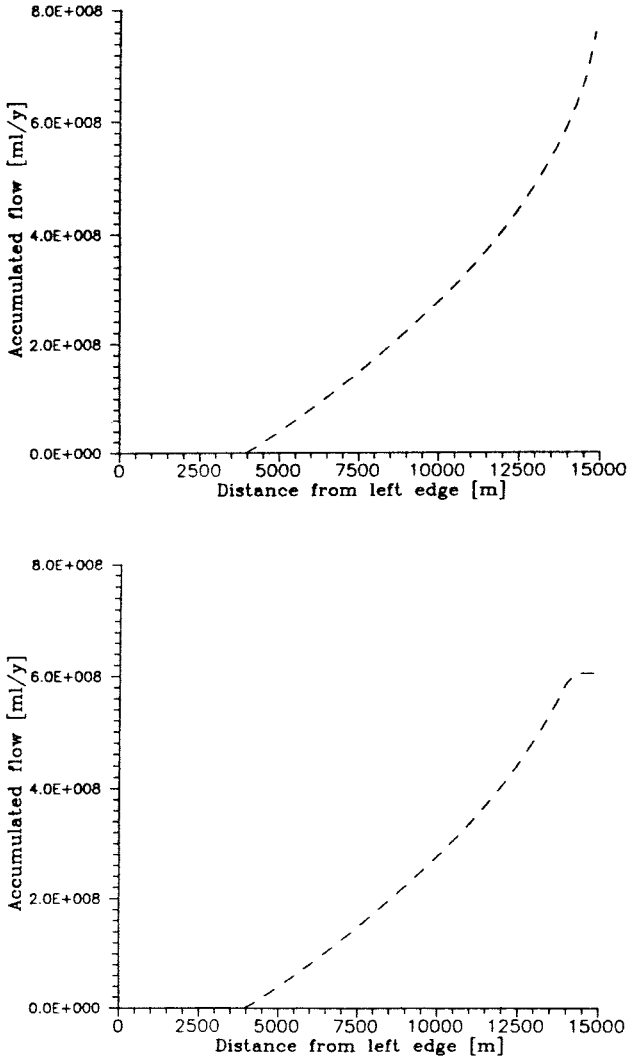

Figure 5.8 Integrated total flow over the top part of the inlet area of Case 1 (upper) and Case 1P (lower).

5.3 Case 2 and Case 2P

5.3.1 Particle Tracking

Figures 5.9 and 5.10 illustrates particle tracks when the particles were released at the same positions as for Case 1 and Case 1P. When comparing these two figures, the presence of the permafrost is qualitatively easy to distinguish. Two features differ between these two cases and Cases 1 and 1P:

- particle 1 takes a much deeper travel path through the domain for Cases 2 and 2P, than was the situation for Cases 1 and 1P (see Figures 5.1 and 5.2), and
- particle 1 takes a deeper and longer travel path in Case 2P than in Case 2, which seems to be appropriate. This was not the situation for Case 1P when compared to Case 1.

The general impression is that the particle tracks behave as expected, i.e. all particles in Case 2P are by the permafrost forced to take longer travel paths through the domain, but that they have smoother shapes than for Cases 1 and 1P. This probably depends on the higher gradients prevailing in the very proximity of the ice-front for Cases 2 and 2P, than was the situation for Cases 1 and 1P. This increase in gradient is a consequence of the steep pressure boundary condition in this area.

Figure 5.11 shows the accumulated travel times for a swarm of particles released at the line at 500 m depth. The retarding effect from the permafrost layer is evident, with a lowering of the travel times of about two orders of magnitude in the vicinity of the ice-front. When the permafrost is not present, i.e. Case 2, the travel times are extremely short with values of about only a few years if a porosity of for instance 10^{-4} is assumed. Also for this case, as well as for Cases 1 and 1P, there is a retarding effect from the permafrost also beyond the extent of it. However, the lowering is limited to be about half an order of magnitude. The bulk of the pathlines appear to have an average travel time of about 100 years assuming a porosity of 10^{-4}, with extremely low values at positions below the ice-front.

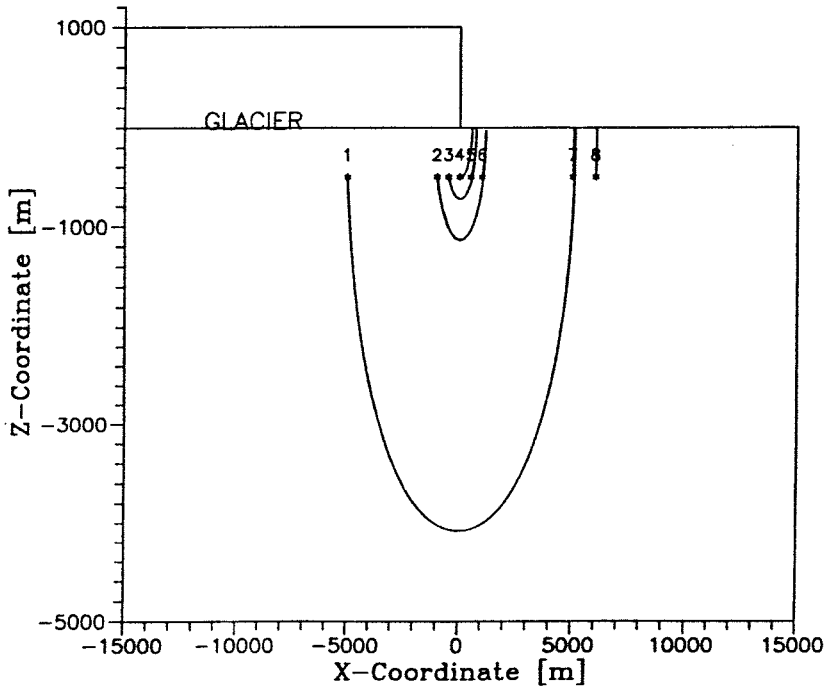

Figure 5.9 Particle tracks as generated for Case 2 (no permafrost).

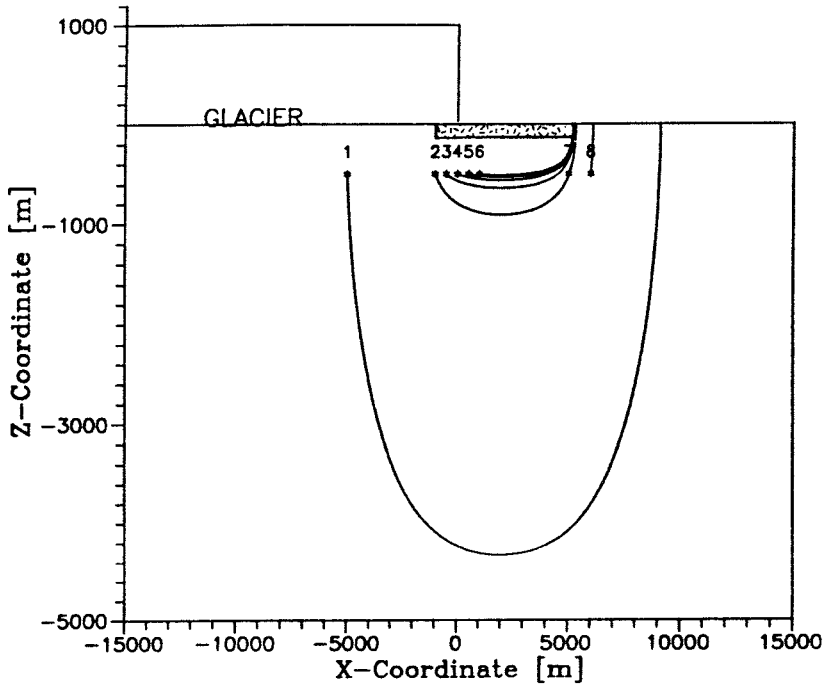

Figure 5.10 Particle tracks as generated for Case 2P (permafrost).

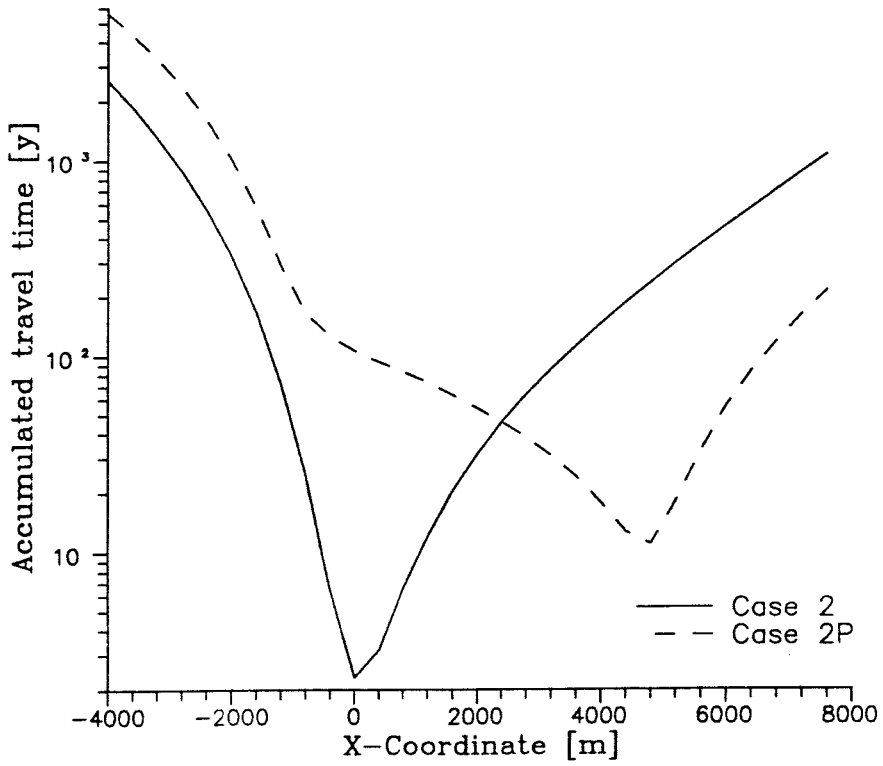

Figure 5.11 Travel times as a function of position for particles released along a horizontal line for Case 2 and Case 2P. A porosity of $1.0 \cdot 10^{-4}$ has been assumed.

5.3.1 Flux Distribution

Figure 5.12 shows the flux distribution along a horizontal line at 500 m depth for Cases 2 and 2P. Note, that the scaling of the y-axis is different from that in Figure 5.7 (Cases 1 and 1P). The peak behaviour is even more pronounced for Cases 2 and 2P than for Cases 1 and 1P, which is a consequence of the extremely sharp gradient just at the position of the ice-front, particularly for Case 2 without permafrost with peak values of about $35 \cdot 10^{-3}$ m^3/m^2/year. This value is about one order of magnitude higher than for Case 1. The retarding effect caused by the permafrost indicates peak values of about $5 \cdot 10^{-3}$ m^3/m^2/year, which also is substantially higher than corresponding situation for Case 1P.

The explanation to this extreme peak behaviour is the extreme gradient imposed just by the ice-front, which brings to the attention the numerical quality of the solution for Case 2 and Case 2P. This can be questioned, since the imposed gradient that contributes to the flow is 1000 m over a few tens of metres (located at the ice-front). It is doubtful if there is a finite element code in the area of groundwater flow modelling (or any other area) that can cope with such sharp gradients with a reasonably maintained quality of the solution.

Figure 5.12 reveals that the contribution of infiltrating water from the ice-sheet located at distances farther away than about 5 km from the ice-front, is nearly equal to zero. This leads to the conclusion that it is not worthwhile calculating the melting water contribution with a pressure boundary condition applied at the top surface, when the ice-sheet and the ground topography are flat, since the driving force for the fluid (i.e. the gradient) is identical equal to zero under such circumstances. This in turn leads to the conclusion that the approach taken with a cut-off in the lateral direction of the ice-sheet when fully evolved as been done for Case 1 and Case 1P, seems to be feasible. The type of boundary condition may be argued since it does not allow for water to infiltrate along the part of the glacier that is not considered, i.e. from the point where the glacier is fully evolved to the core of the glacier; a "flat" area. However, if using an imposed infiltration rate as opposed to a prescribed pressure boundary, it has to be given a direction, in this case directed vertically downwards. But, once the infiltrated water has entered the domain, a gradient is still a prerequisite for flow to take place. Since the topography is flat, this strategy would not have implied an increase in infiltrated melting water. The only measure to be taken for this part of the glacier, would be to impose either a sloping ground surface or an infiltration rate not being directed vertically downwards.

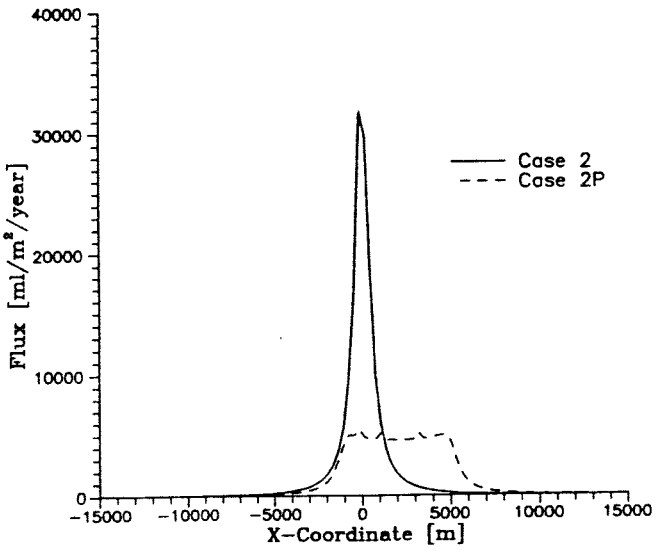

Figure 5.12 Flux values (ml/m^2/year) along a line at 500 m depth for Case 2 and Case 2P.

6. Summing up – Conclusions – Future Work

Since the present study has to be regarded as "exploratory", a major attention is brought to the phenomena studied, at the expense of elaborate discussions on the actual conditions at the site. Therefore, the values pointed at and discussed below should be regarded as a guidance in order to shed light on orders of magnitude. However, five major conclusions or comments for future work can be stated on the basis of the results from the present study. Some of the issues related to the conclusions are coupled, but in a general sense the conclusions can be classified accordingly:

- Large amounts of water infiltrate into the domain due to the melting away of ice. The major part of the water enters the domain in the vicinity of the ice-front where the hydraulic gradients are largest. As a consequence of the posed geometry and boundary conditions, large amounts of water are discharged on the outlet side in the very neighbourhood of the ice-front. A pronounced peak behaviour of the system can be observed, which indicates that the distance over which the water is discharged is limited to a few kilometres. The main cases were concerned with a pressure boundary condition corresponding to the shape of the ice-sheet that was applied along the top surface (Case 1 and Case 1P), with hydraulic conductivities according to data from the Finnsjön-site. The fluxes for these cases at a depth of 500 m reached peak values of about $4 \cdot 10^{-3}$ $m^3/m^2/year$.

  Neither of the cases studied indicated that the presence of permafrost would imply dramatic effects on the groundwater flow. When present, the effects from the permafrost appeared to be retarding in the area below the ice-front, whereas the flow at the edge of the permafrost layer was increased by roughly a factor of 10, or conversely, the travel times of particles released at 500 m depth were shortened by a factor of 10 due to the permafrost in this particular area.

- Two sets of cases have been concerned with the presence of a pressure boundary condition with a shape corresponding to that of an ice-sheet. This has lead to a continuous build-up of a gradient over the inlet part of the domain, which was not the case with an evenly distributed pressure imposed along the top boundary. The latter showed that water entered the domain only at the very neighbourhood of the ice-front, an area where a gradient of 1000 m over a few tens of metres was imposed, and practically no water at all entered the domain in the area closer to the core of the glacier.

- Particularly the case discussed above with a flat pressure profile imposed as a top boundary condition, implied that enormous gradients were at hand at the ice-front. Due to this, a warning is raised against the numerical solution of the results in this area of the domain. As was shown for one of the cases, the calculated flux along the top surface could be dependent on the grid resolution; an even finer discretisation may imply that the values of the fluxes in this particular "high gradient region" may differ again. However, there is no reason to believe that the results from the modelling exercise as a whole would suffer from numerical uncertainties; these seem to be located in a narrow region around the ice-front.

- Despite that the project has shed light on some interesting phenomena related to the performance of a potential repository during a de-glaciation phase, there are some conceptual uncertainties that should be mentioned. These could for instance be the hydraulic conductivity of the host rock when being severely compressed by the ice-burden, internal fracturing in the ice-sheet due to run-off of melting water and high pressures, the closing or widening-up of fracture zones being subject to high pressures from partly the ice-sheet itself and partly by the pressure from the melting water, the porosity of the host rock when being compressed, which affects the travel times for

particles escaping from the repository, the effect on the geological barrier from the potential crustal downwarping, etc, etc.

- Despite the conceptual uncertainties, the uncertainties in input data, and possible numerical instabilities in the vicinity of the ice-front, a reasonable degree of confidence could be put into the results. This statement is based on the results from the calculation of total flow along the top boundary, which appeared to be in amazingly good agreement with the values that initially were discussed as the geothermal melting capacity. Of course, the calculated flow is a function of the hydraulic conductivities assigned to the bedrock. Nevertheless, the results seem to indicate values that at least are in the right order of magnitude under the circumstances, and by this one can state the approach taken seems to hold, at least serving as a basis for future studies in the area of glaciations and the extreme flow conditions that prevail during the de-glaciation phase. These could be oriented towards studies addressing the conceptual uncertainties as mentioned above.

References

Ahlbom K, Äikäs T, Ericsson L O, 1991,
"SKB/TVO Ice age scenario", SKB Technical Report TR 91-32, Swedish Nuclear Fuel and Waste Management Company (SKB), Stockholm, Sweden.

Andersson J-E, Nordqvist R, Nyberg G, Smellie J, Tirén S, 1991,
"Hydrogeological conditions in the Finnsjön area; Compilation of data and conceptual model", SKB Technical Report TR 91-24, Swedish Nuclear Fuel and Waste Management Company, Stockholm, Sweden.

Atkinson R, Herbert A, Jackson C P, Robinson P C, 1985,
"Nammu User's Guide", Report AERE R-11364, Atomic Energy Research Establishment, Harwell Laboratory, United Kingdom.

Boulton G, 1991,
Correspondence between prof. G. Boulton and SKB, 1991.

Embleton C, King C A M, 1975,
"Glacial Geomorphology", Published by Edward Arnolds Ltd., London, England.

Pusch R, Börgesson L, Knutsson S, 1990,
"Origin of silty fracture fillings in crystalline bedrock", GFF Vol 112, part 3, pp 209-213, The Geological Society of Sweden.

Grundfelt B, Boghammar A, Lindberg H, 1989,
"HYPAC User's Guide", Working Report AR 89-22, Swedish Nuclear Fuel and Waste Management Co., Stockholm, Sweden.

Rae J, Robinson P C, 1979,
"NAMMU: Finite-element program for coupled heat and groundwater flow problems", Report AERE R-9610, Atomic Energy Research Establishment, Harwell Laboratory, United Kingdom.

Rosengren L, Stephansson O, 1990,
"Distinct element modelling of the rock mass response to glaciation at Finnsjön, central Sweden", SKB Technical Report TR 90-40, Swedish Nuclear Fuel and Waste Management Company (SKB), Stockholm, Sweden.

APPENDIX A

An initial study of permafrost influences on the groundwater flow at the Finnsjön site

Contents:

A1. Introduction

On the basis of what has been reported in the main report within the present project, there was an interest to study the potential impact from permafrost-like conditions at the Finnsjön site. The calculations have to be regarded as semi-generic, since there are data available in terms of fracture zone conductivities, rock mass conductivities, reasonable assumptions with regard to porosities etc. under undisturbed "normal" conditions; but, there are some major conceptual uncertainties that still remain to be investigated and analysed. These are mainly concerned with the mechanical impact on the rock mass and the fracture zones that can be expected from an ice-sheet, and to what degree the overburden affects the conductivities and porosities, and so on. Despite these uncertainties, one could possibly claim that the conditions assumed here are not associated with more conceptual uncertainties than ordinary groundwater flow calculations, since it is generally recognised that a glaciation is preceded by tundra-like conditions followed by an evolution of permafrost prior to the evolution of the glacier itself. Hence, the permafrost situation considered here may reflect the conditions similar to those that are expected prior to the evolution of the ice-sheet during next glaciation, which would imply that the conceptual uncertainties mentioned above, at least to some extent are reduced.

The calculations made use of the NAMMU-code (Rae J, et al, 1979, and Atkinson R, et al, 1985), for solving the equation system, while the HYPAC-program package (Grundfelt, B et al, 1989) was used for pre- and postprocessing purposes.

A2. Boundary Conditions and Hydraulic Properties

The conceptual basis for the model set-up is a two-dimensional vertical cross-section reported in (Andersson J-E, et al, 1991), which is shown in Figure A1. This vertical cut was also used in (Lindbom B, et al, 1991) for other purposes than those in the present study. The area to the left of zone 12 has been extended in the present study if compared to the vertical cross section described in (Lindbom B, et al, 1991). This implies that the domain now includes zone 14, and furthermore, this extended area has a flat topography. The reason for extending the domain, was that the permafrost, as will be shown later in this paper, is assumed to be located at different depths in the area between zones 1 and 12. To avoid the situation of a zero-gradient and hereby "artificially" stagnant water as a consequence of the presence of the permafrost, this measure was taken (i.e. to maintain a driving force for the fluid). The driving force for the groundwater flow is the topographic gradient over the top surface above zone 2, a difference in height of 3 m over the entire region, or correspondingly about 0.7%.

Four different cases have been studied that differ only in terms of the vertical extent of the permafrost. The hydraulic conductivities for these cases do not differ internally, nor do the boundary conditions. The four cases will from now on be referred to as Cases PF1-PF4.

The boundary conditions for the two-dimensional cross-section are of no-flow type for the lateral and bottom boundaries. The top boundary coincides with the groundwater table and is regarded as a "zero-pressure" boundary.

Table A1 shows the hydraulic conductivities as assigned to the fracture zones. The rock mass conductivity is the same as used in (Lindbom B, et al, 1991), i.e. $K=1.06 \cdot 10^{-6} \cdot z^{-1.1}$. The conductivity of the permafrost is taken be equal to zero. However, in order not to obtain numerical instabilities in NAMMU, the conductivity of the permafrost has been assigned the value $K=10^{-15}$ m/s, which can be regarded as impervious in this context.

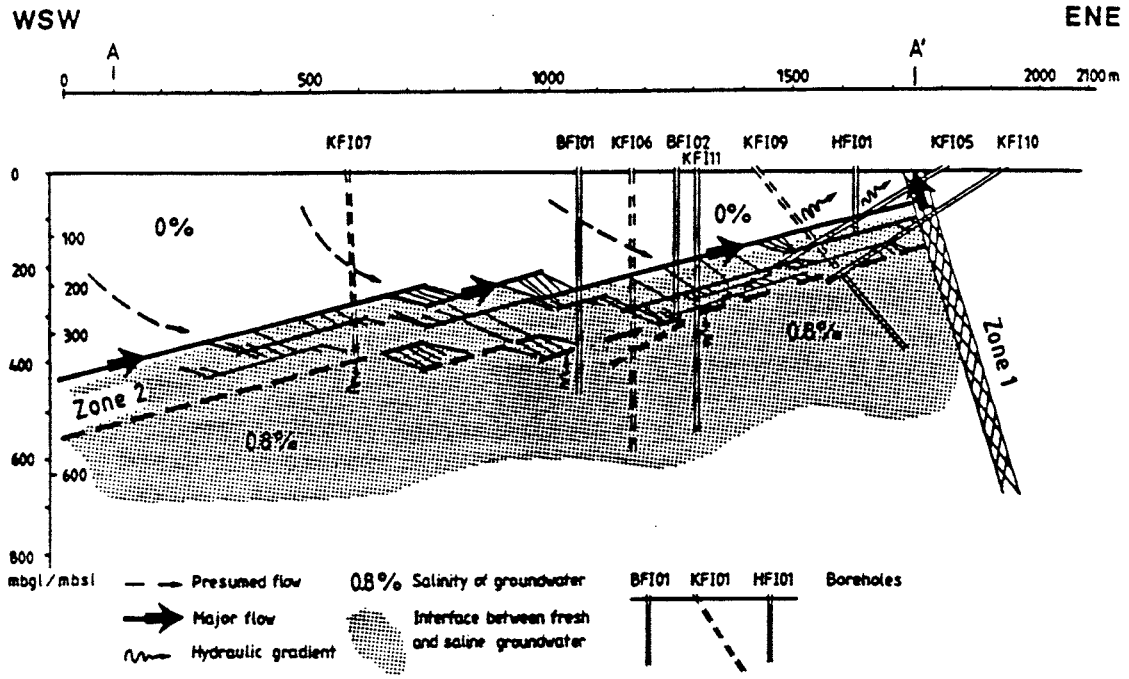

Figure A1 *Conceptual basis for the present study with a vertical view crossing zone 2 (From Andersson J-E, et al, 1991).*

Table A1 *Fracture zones in the Finnsjön area as modelled within the study.*

Zone	Width (m)	Inclination (degrees)	K (m/s)
1	20	75	$1.21 \cdot 10^{-3} \cdot z^{-1.1}$
2	100	16	$1.02 \cdot 10^{-2} \cdot z^{-1.1}$
12	50	90	$3.70 \cdot 10^{-4} \cdot z^{-1.1}$
14	50	90	$3.70 \cdot 10^{-4} \cdot z^{-1.1}$

The nomenclature and features of the four cases that were studied are listed below.

Case PF1: This is the initial case for the permafrost study, and it assumes that the permafrost is yet non-existing.

Case PF2: The permafrost is assumed to reach to a level between zone 2 and the ground surface between zone 1 and zone 12, about 250 m below ground surface to about 50 m below ground surface; apart from that the case is identical to Case PF1.

Case PF3: The permafrost is assumed to reach down to the lower limit of zone 2; apart from that identical to Case PF1.

Case PF4: The permafrost is assumed to reach down to a level of about 700 m, i.e. below repository level. Apart from that identical to Case PF1.

A3. Modelling Results – Discussion and Conclusions

The evaluation includes contour diagrams of the fluxes and tracking of particles for the four cases. In addition, typical flux values in the potential repository are reported for each of the cases, as well as typical travel times and travel lengths for particle trajectories. The repository is assumed to be located between 400 m and 1400 m in the x-direction at 600 m depth.

The modelling results presented in this Appendix have shown that the permafrost well may act as an effective barrier once the permafrost has reached down to levels well below zone 2; levels of around 700 m below ground surface. The earlier stage of permafrost (permafrost down to a level of about 200 m indicated that no retarding influences at all could be seen either at fluxes at repository level, or at particle tracks released within the domain. As a matter of fact, the fluxes were seen to be a bit higher than the fresh-water situation when the permafrost penetrated down to a level coinciding with the lower confinement of zone 2, which was caused by a plugging of the natural discharge paths in zone 2, and the part of rock located above zone 2.

Figures A2-A5 show the flux distribution for the four cases studied. The assumed extent of the permafrost is indicated as a dark area between zone 1 and zone 12. Case PF1 is the reference case with no permafrost.

The fluxes at repository level under natural conditions amounted to about 5 ml/m^2/year ($5 \cdot 10^{-6}$ m^3/m^2/year), with roughly the same value for the case when the permafrost reached to a level of about 200 m, see Figures A2-A3. The fluxes just below zone 2 are at least three orders of magnitude lower than those in it for both these situations, reflecting the contrast in hydraulic conductivity between the rock mass and zone 2. When the permafrost was assumed to coincide with the lower boundary of zone 2, the fluxes were in the order of about 40 ml/m^2/year ($4 \cdot 10^{-5}$ m^3/m^2/year), see Figure A4. For this case, the top boundary condition at the left hand side over zones 12 and 14 implies that the imposed water still is forced to the right hand boundary and ought to lead to an increase of the fluxes below zone 2. This increase is however not visible in the contouring of the fluxes since this is based on an interpolation scheme, which was not capable of detecting local features. One of these is for instance the flux through the potential repository. The plugging of zone 2 has thus in this case lead to an increase of the flux through the repository.

A somewhat different result can be seen for Case PF4 in Figure A5. The "plugging" of the domain to such large extent as shown, lowers the flux through the entire domain, which leads to stagnant water not only in the permafrost but also in the parts beneath the permafrost. Flow takes place only in the fracture zones, and is limited even here.

For the particle tracking, the intention was to have two particles released at both ends of the potential repository, while six particles were to be released in the rock mass between the left hand boundary and zone 12 in order to trace the flow paths from the recharge area. This approach was feasible for Cases PF1 and PF2 (see Figures A6 and A7), but when the permafrost was assumed to have penetrated deeper down in the domain as in Cases PF3 and PF4 (see Figures A8 and A9), the gradient in the recharge part of the domain was too small to allow for particles to be transported, they were aborted by the tracking routine. In order to "force" the particles to move, the release points were thus moved for these two cases to the inner and upper part of zone 12, where the gradients were assumed to be higher than in the surrounding rock.

The particle tracking showed further evidence for the vertical separation of the flow domain caused by zone 2 and its interaction with the bounding fracture zones. The case with no permafrost showed that the particles, regardless of release position, were discharged in zone 1 via zone 2. The situation with permafrost down to the lower confinement of zone 2 showed that the particles in this case were discharged through the bedrock to zone 1. This was not entirely caused by the presence of the permafrost itself, but rather to the fact that the permafrost reduced the gradient over the domain, so that the driving force for the fluid was substantially reduced, and even more, the particles

appeared to be easily aborted due to this. The latter case showed travel times (porosity = 10^{-4}) of around $2 \cdot 10^3$ years from the repository, whereas the two former cases had travel times of around $1\text{-}5 \cdot 10^3$ years. The travel times for the remaining particles, i.e. those released outside the repository, had travel times of roughly 60 years for the two former cases, while the case with permafrost down to the lower limit of zone 2 had travel times of around $5 \cdot 10^3$ years. The case with permafrost showed travel times that indicated stagnant water within the permafrost, although the particles amazingly enough were not aborted by the tracking routine. The remaining particles for this case showed travel times of around 10^4 years.

The initial calculations presented in this Appendix do not consider the de-glaciation phase, as opposed to what was dealt with in the main part of the study. Thus, the recession of the permafrost is not considered, nor is the presence of melting water. Rather, the interest has been focussed on the evolution of the permafrost prior to the evolution of the ice-sheet, at different positions in time, and the degree of impact on fluxes at repository level and particle tracking that can be expected from the permafrost. Whether or not the permafrost can be regarded as a barrier for escaping radionuclides is entirely depending on the longevity of the permafrost, i.e. the time elapsed from the point in time of the isolation of the repository by the permafrost, to the time of a glacier recession or development.

The integrity of the permafrost barrier may be questioned if the heat from the repository is high enough. If counting on the permafrost as an active barrier, the heat decay should therefore be penetrated in future studies in order to establish an understanding as to what point in time the heat from the repository is low enough not to affect the permafrost barrier. The reason for this concern is the potential risk for melting permafrost due to the heat from the repository. In the main study within the present study, it was shown that the high flows will occur over short time periods, provided that a source with water is present which feeds the flow system.

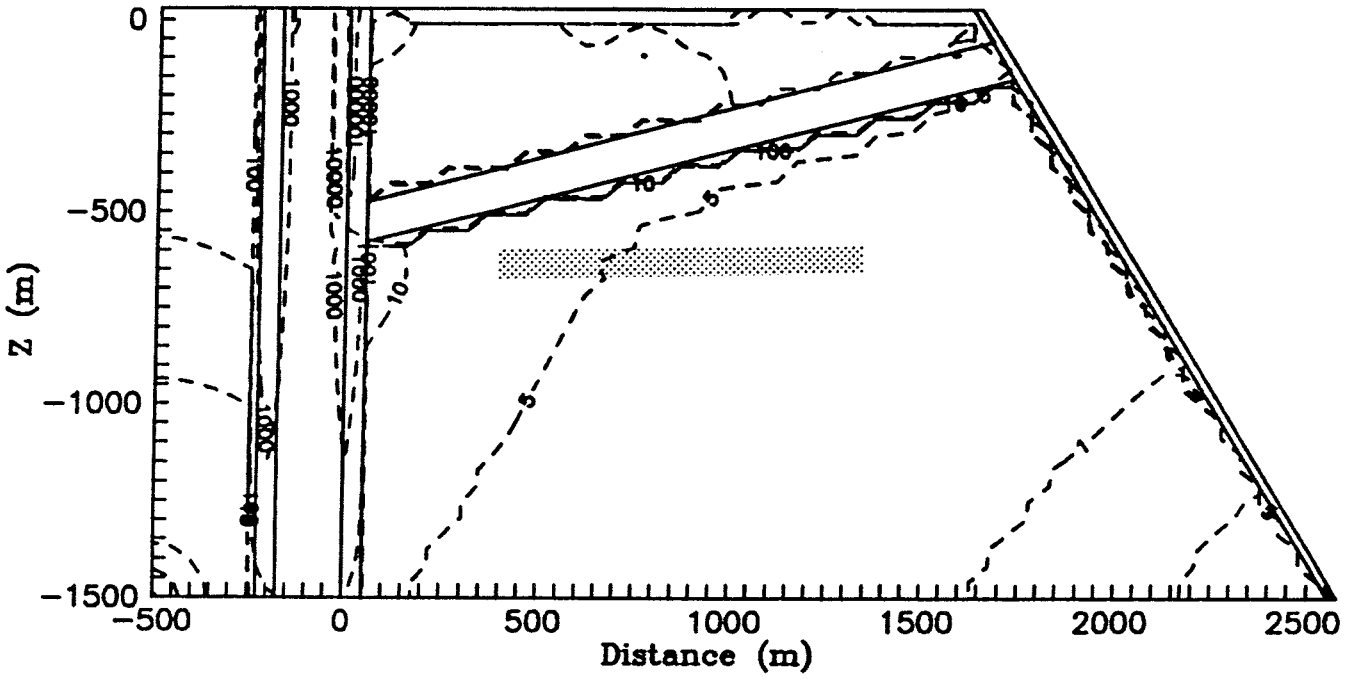

Figure A2 *Flux distribution (ml/m²/year) for Case PF1. The repository area is shaded.*

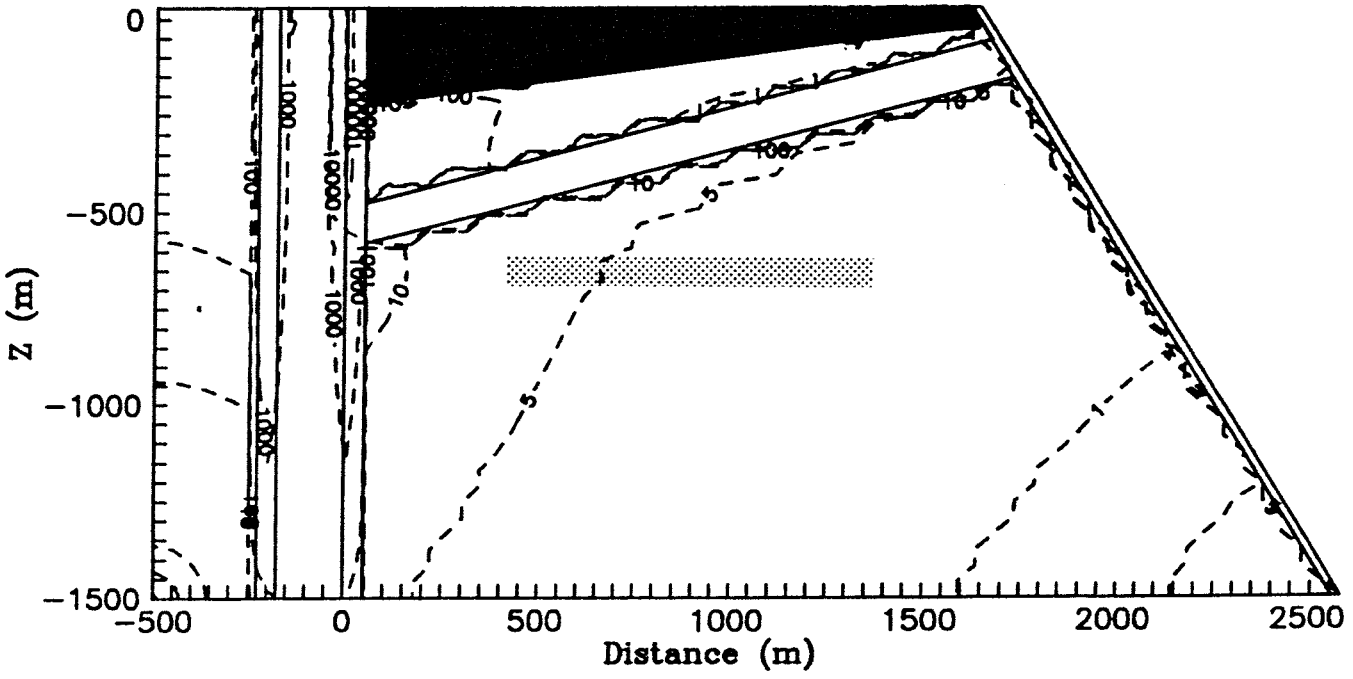

Figure A3 *Flux distribution (ml/m²/year) for Case PF2. The repository area is shaded.*

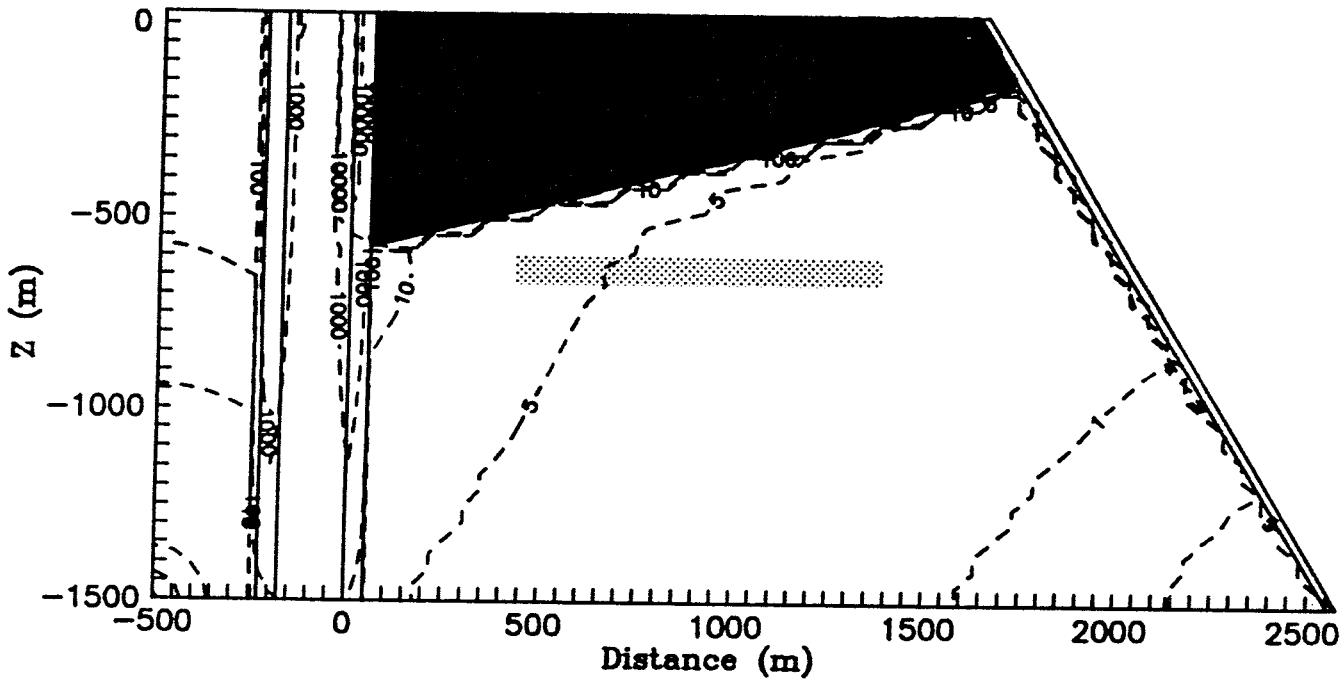

Figure A4 *Flux distribution (ml/m²/year) for Case PF3. The repository area is shaded.*

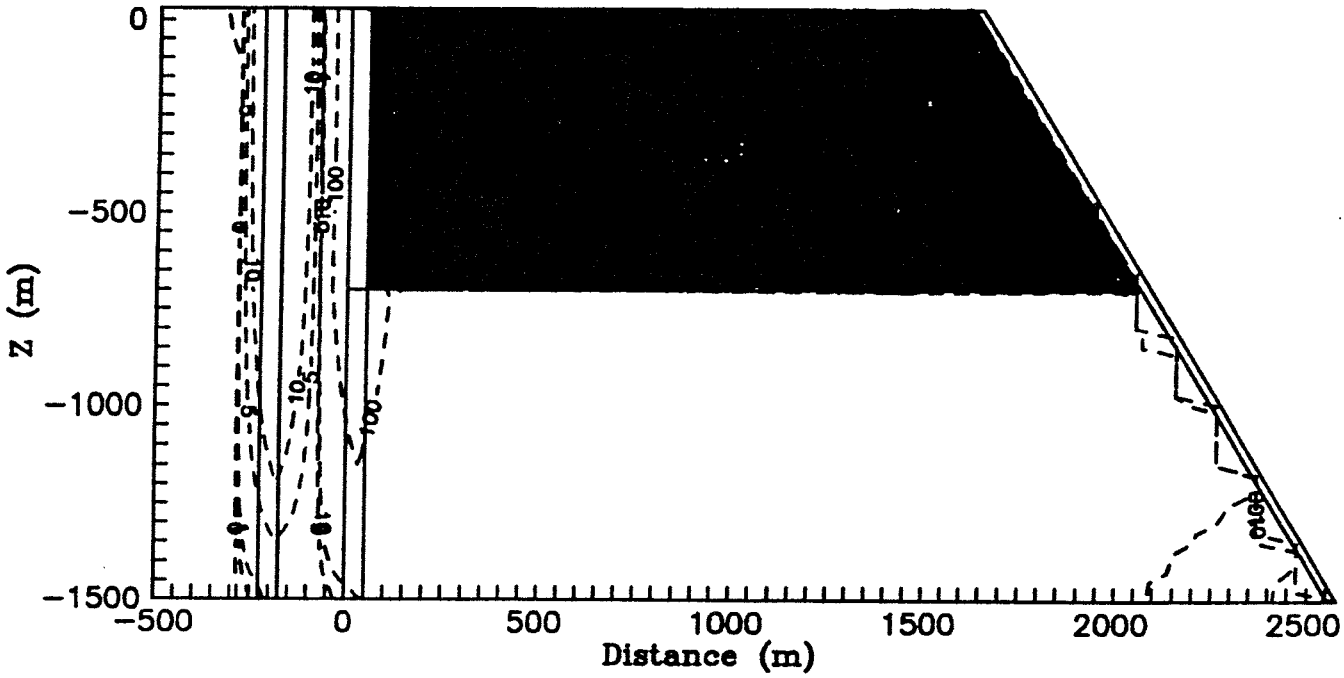

Figure A5 *Flux distribution (ml/m²/year) for Case PF4.*

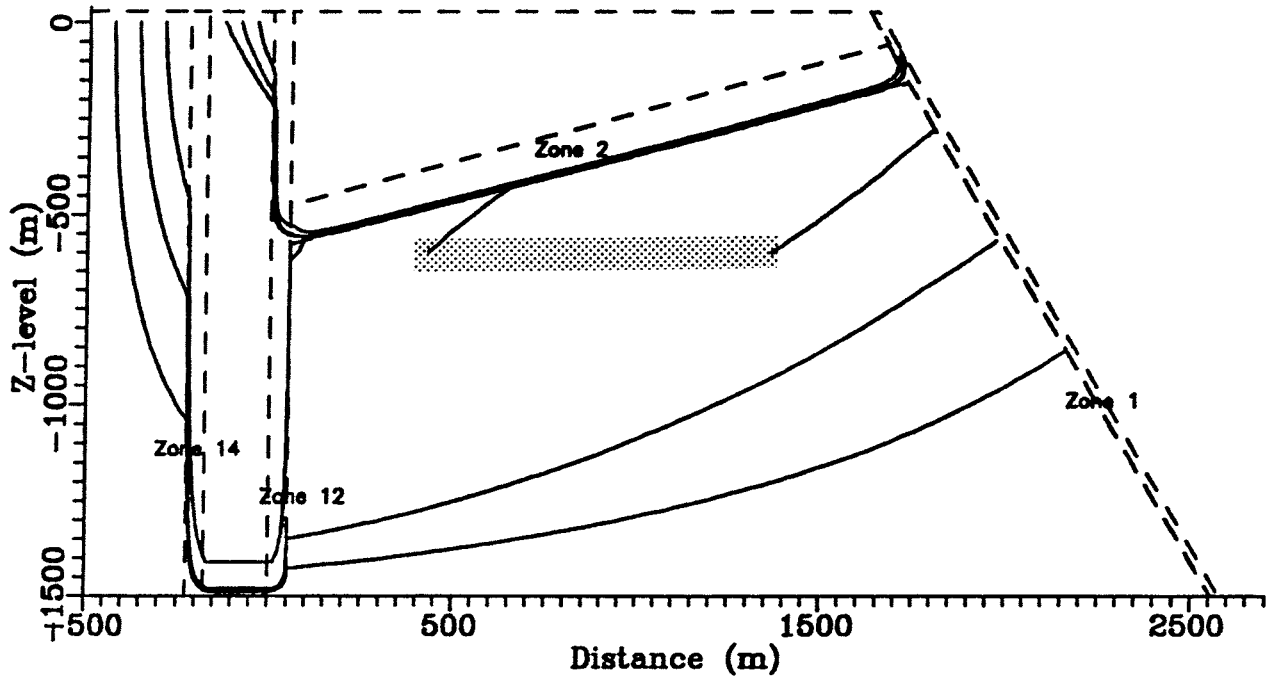

Figure A6 *Particle tracks for Case PF1. The repository area is shaded.*

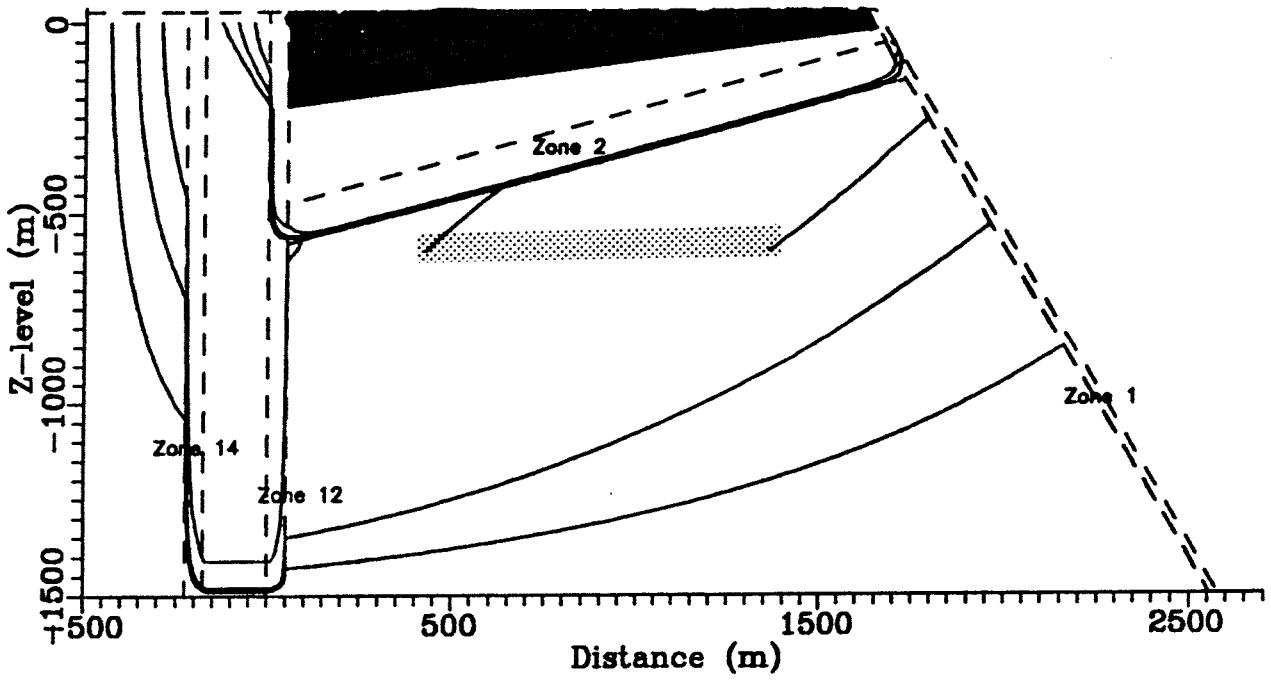

Figure A7 *Particle tracks for Case PF2. The repository area is shaded.*

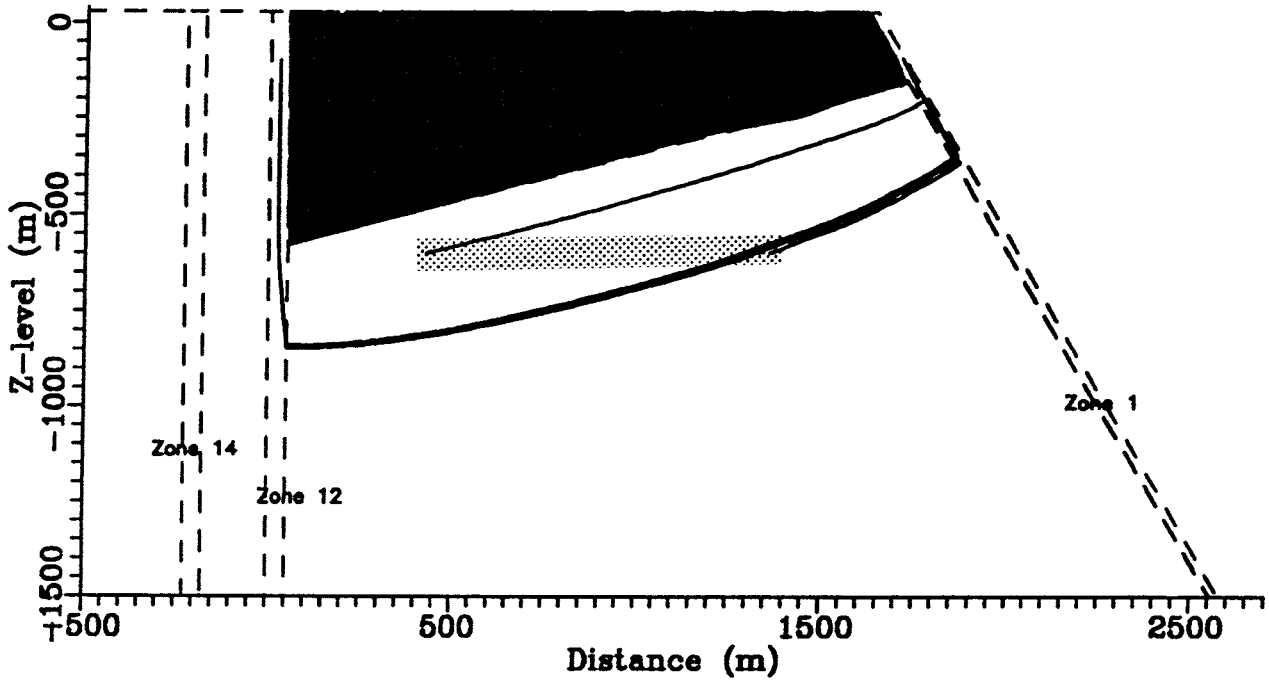

Figure A8 *Particle tracks for Case PF3. The repository area is shaded.*

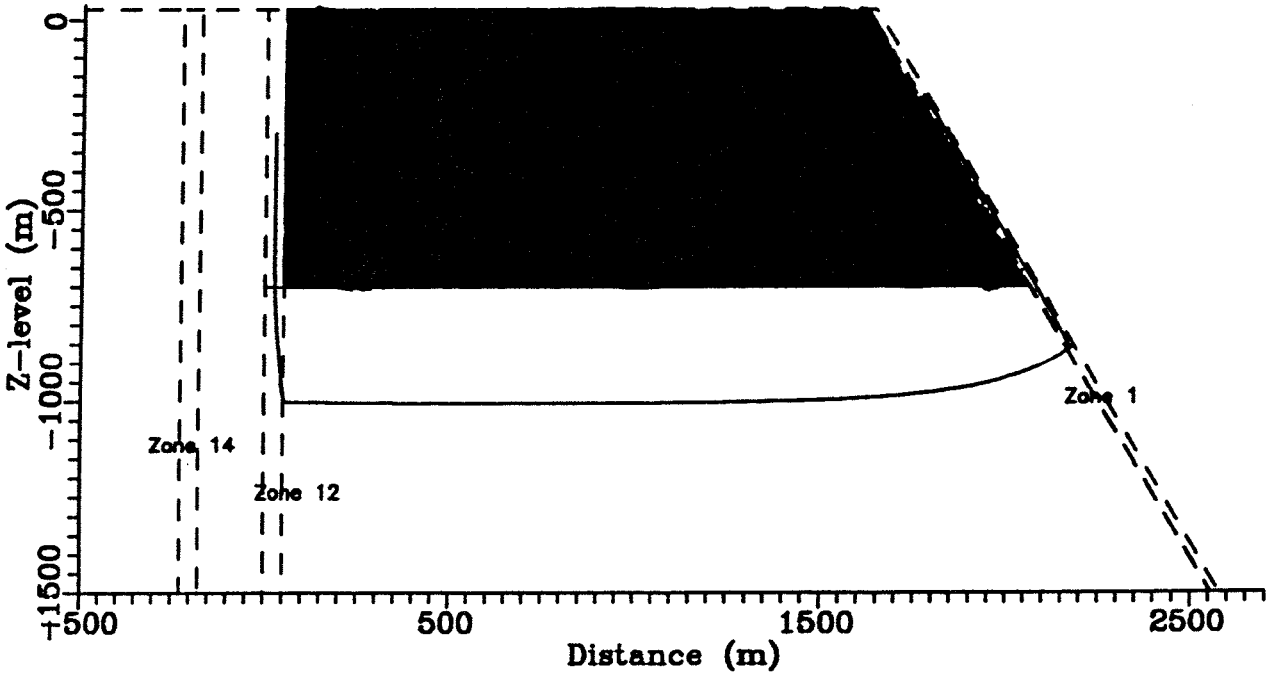

Figure A9 *Particle tracks for Case PF4.*

References to Appendix A

Rae J., P.C. Robinson, 1979,
"NAMMU: Finite-Element program for coupled heat and groundwater flow problems", Report AERE R-9610, U.K. Atomic Energy Research Establishment, Harwell Laboratory, United Kingdom.

Atkinson R., A.W. Herbert, C.P. Jackson, P.C. Robinson, 1985,
"NAMMU User Guide", Report AERE R-11364, U.K. Atomic Energy Research Establishment, Harwell Laboratory, United Kingdom.

Andersson J-E, Nordqvist R, Nyberg G, Smellie J, Tirén S, 1991,
"Hydrogeological conditions in the Finnsjön area; Compilation of data and conceptual model", SKB Technical Report TR 91-24, Swedish Nuclear Fuel and Waste Management Company, Stockholm, Sweden.

Lindbom B, Boghammar A, Lindberg H, Bjelkås J, 1991,
"Numerical groundwater flow calculations at the Finnsjön site", SKB Technical Report TR 91-12, Swedish Nuclear Fuel and Waste Management Company, Stockholm, Sweden.

Grundfelt, B., A. Boghammar, H. Lindberg, 1989
"HYPAC User's Guide", Working Report 89-22, Swedish Nuclear Fuel and Waste Management Company, Stockholm, Sweden.

APPENDIX B

Transfer of lateral boundary pressures from full scale glacier model to local scale glacier model

Contents:

B1 Introduction

This appendix deals with the regional scale modelling that preceded the calculations that were reported in the main report. The underlying objective with this pre-study was to reduce the domain, from the scale of hundreds of kilometres to tens of kilometres, in order to increase the discretisation on the reduced scale models. The basic idea with this, was to investigate whether or not the groundwater flow could be affected by the position of the lateral boundary in the outlet area in a reduced model. Assuming that this boundary would be regarded as a no-flow boundary, the distance from the ice-front to this boundary could have an impact on the results since this is the very outlet area, subjected to rather extreme conditions at the inlet area. It is therefore essential to demonstrate that the position of this lateral boundary is located well away from the outlet point for the water, not to affect the flow situation. Furthermore, there was a wish to reduce the domain, mainly from the point of view of computational savings.

The approach was as follows: Consider the length of the glacier from the ice-front to the point in the horizontal direction where the ice-sheet has reached its maximum. Let the domain expand equally much at the other side of the ice-front. This makes the entire length of the modelled domain be 220 km, 110 km on each side of the ice-front, a distance corresponding to a fully evolved ice-sheet of 1500 m at the inlet side. Now, let this geometry define what we may call a full scale model. The driving force from hydraulic point of view is the ice-sheet, which is imposed along the top boundary as a pressure boundary condition. The lateral confinements are treated as no-flow boundaries as well as the bottom boundary.

Two vertical profiles, later intended to confine the reduced domain, were arbitrarily chosen at a distance of 15 km at each side of the ice-front at the inlet side. By transferring the pressure distribution in a vertical profile at 15 km distance at the inlet side from the ice-front as calculated in a full scale model, a pressure boundary condition could be prescribed for the cases calculated with a reduced domain. Accordingly, at the outlet side of the domain, the interest was focussed on the flow distribution along the vertical profile at a distance 15 km beyond the ice-front. If this flow is small enough compared to the inlet flow, it would justify the location of a lateral no-flow boundary at this position. The lateral boundary at the inlet side would by this approach be of a prescribed pressure type being transferred from the full scale model, i.e. the ice-sheet from this lateral boundary to the position where the glacier is fully evolved, is replaced by the pressure being prescribed along the lateral vertical boundary. The benefit from this approach is the possibility to increase the discretisation of the reduced domain. The meshes for the pre-study cases consisted of about 7200 eight-noded quadri-lateral finite elements for the full scale model. The approach taken according to above, implied that one full scale modelling was required for each of the four cases presented in the main report.

Finally, it could be argued that the left-hand lateral boundary is treated as a no-flow boundary since one surely can expect water to penetrate from beyond this boundary to the core of the glacier. However, the contribution of melting water that infiltrates into the bedrock from this part of the glacier is negligible for the present study. This depends on that this "interior" part of the ice-sheet is regarded as flat, implying that the gradient is zero, which in turn means that the flow directed vertically into the domain also has to be regarded as non-existing. This could perhaps not be considered as a true reflection of the conditions in nature. However, large amounts of melting water can be expected beneath the ice-sheet, but the major part of this water, stemming from the part of the ice-sheet that is not modelled in the full scale model, is discharged horizontally and thus, it does not contribute to a flow increase in the deeper parts of the bedrock. This would at least to some extent justify the approach taken here.

The hydraulic properties of the bedrock are equal to those in the main report, $K=1.0\cdot10^{-6}\cdot z^{-1.1}$ m/s.

B2 Regional Scale Modelling Preceding Case 1 Case 1P

Figure B1 illustrates the flow along the vertical profiles located at 15 km and 30 on each side of the ice-front. As opposed to the situation shown in Figure B1, a permafrost layer of 100 m depth and an extent of 5 km beyond the ice-front has been assumed in Figure B2. The results presented in both figures are based on the full scale model extending 110 km on each side of the ice-front. These figures show that only a very small portion of the flow is discharged through the profile located at 15 km beyond the ice-front. In fact, 99.9 % of the water has been discharged prior to this location, which could be seen as an evidence of that a location of the lateral boundary at the outlet side will not affect the flow situation. By prescribing a pressure boundary condition at the lateral inlet side (transferred from the full scale model) to Case 1 and 1P, and by prescribing a no-flow boundary at the outlet lateral confinement, the geometry and boundary conditions are established for Cases 1 and 1P.

In order to further confirm that the flow on the outlet side probably will be concentrated to the vicinity of the ice-front, the flux distribution along the top boundary over the entire domain for the full scale model was calculated for a case without permafrost. Figure B3 reveals three important features: *i)* the flow beneath the ice-sheet is almost constant to a specific point at roughly 30 km distance from the ice-front, where it increases dramatically at the very neighbourhood of the ice-front, *ii)* the discharge is extremely concentrated to the absolute neighbourhood of the ice-front, but at the outlet side; the flow to the right of for example a profile located at 10 km beyond the ice-front is next to non-existing, and *iii)* the major part of the flow takes place along the ice-sheet, i.e. the horizontal component of the flux is about one order of magnitude larger than the vertical one. This should be seen as a consequence of the infiltration capacity of the bedrock beneath the ice-sheet being too low to allow for larger amounts of water to infiltrate. Furthermore, this could also be seen as a reflection of the processes taking place under natural conditions.

In conclusion, Figures B1-B3 reinforces the impression that a domain being reduced in size along the lines as indicated earlier seems to be feasible.

B3 Regional Scale Modelling Preceding Case 2 Case 2P

The same procedure as shown in Section B2 was repeated for the regional scale modelling preceding Case 2 and Case 2P. These cases are identical to Case 1 and Case 1P, with the exception that the pressure boundary condition in the former two cases is assumed to be evenly distributed with a continuous value equal to 1000 m. This pressure corresponds to an ice-sheet with an average height (of 1000 m) of that modelled in Case 1 and Case 1P. Figure B4 shows the flux along vertical profiles located at a distance of 15 km and 30 km on each side of the ice-front for the full scale model preceding the calculations for Case 2 and Case 2P. There are two important features that differ between this case and Case 1: the first is that the flux values are much smaller at the profiles at 15 km for Case 2 than for Case 1, roughly two-three orders of magnitude, and secondly the fluxes are symmetrically distributed with respect to the ice-front. The latter implied that the approach with a no-flow lateral boundary at the outlet side had to be abandoned, since this approach was based on that the flow at the outlet side had to be significantly lower than at corresponding position at the inlet side. Thus, the only alternative was to transfer the boundary pressures from the full scale model to the models that were to be reduced in size. Since this conclusion was evident for the case without permafrost, the flow distribution corresponding to that in Figure B4 was not calculated for the case with permafrost.

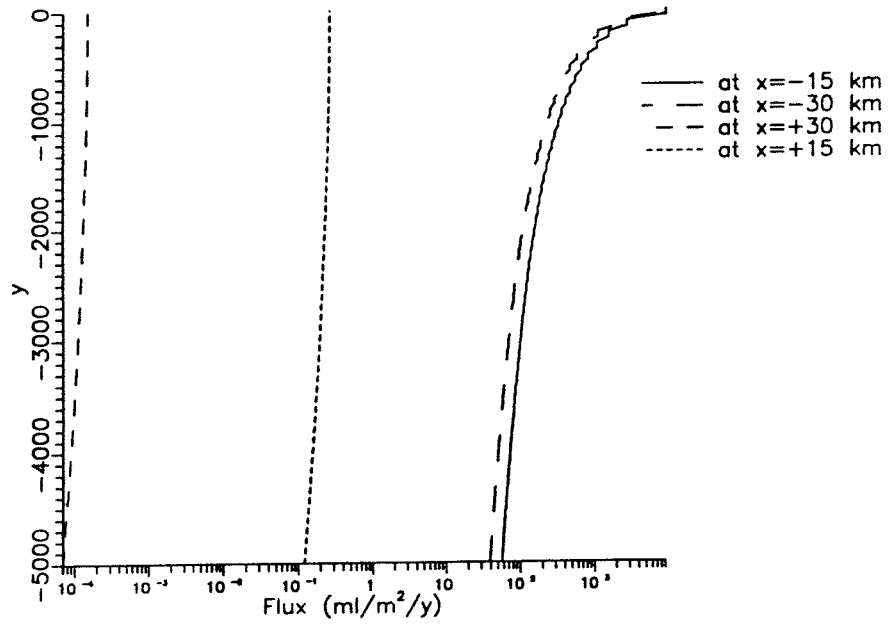

Figure B1 Results from the full scale model: Flux distribution in vertical profiles located at 15 km and 30 km on each side of the ice-front. Top boundary pressure coinciding with the shape of the ice-sheet. No permafrost assumed. Preceding Case 1 and Case 1P.

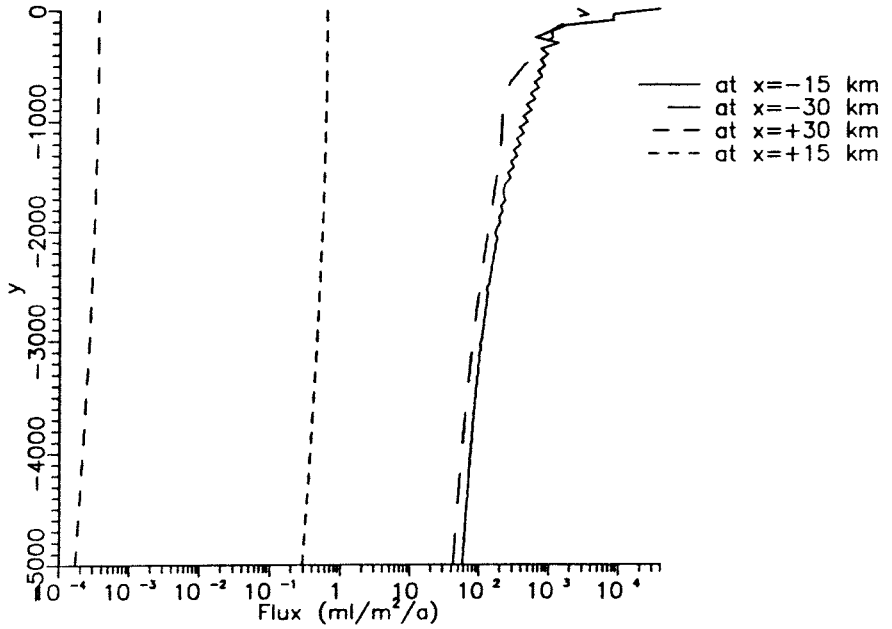

Figure B2 Results from the full scale model: Flux distribution in vertical profiles located at 15 km and 30 km on each side of the ice-front. Top boundary pressure coinciding with the shape of the ice-sheet. Permafrost assumed. Preceding Case 1 and Case 1P.

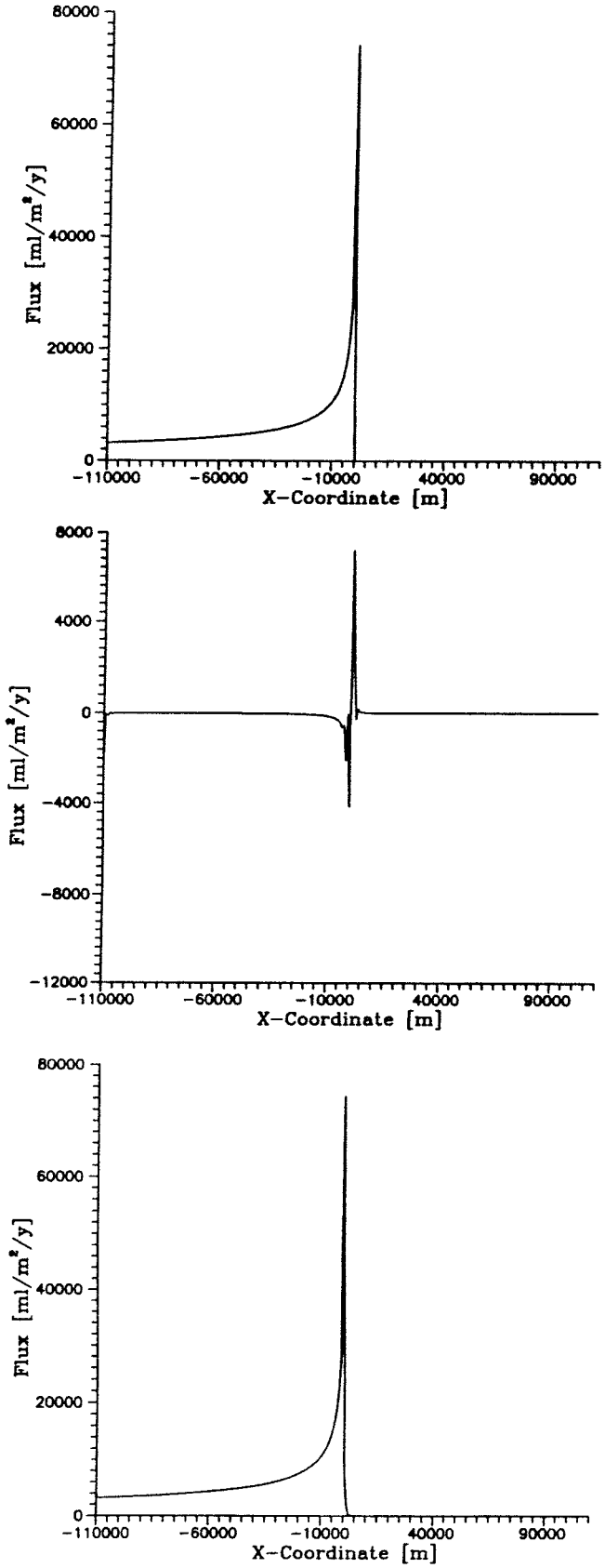

Figure B3 Results from the full scale model: Flux distribution along the top surface over the entire domain. Upper: Horizontal component of flux; Middle: Vertical component of flux; Lower: Total flux. Top boundary pressure coinciding with the shape of the ice-sheet. No permafrost assumed.

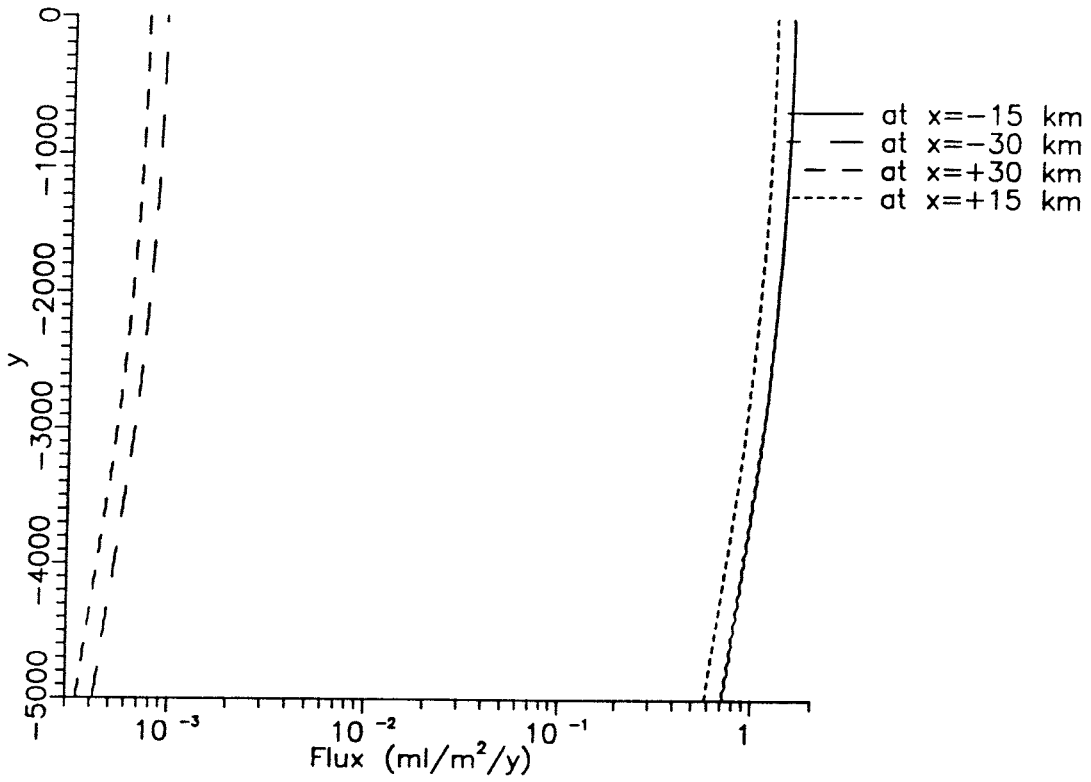

Figure B4 Results from the full scale model: Flux distribution in vertical profiles located at 15 km and 30 km on each side of the ice-front. Top boundary pressure evenly distributed along the top boundary with a constant height of 1000 m. No permafrost assumed.

Documentation of files created and processed during the project

For each case the program sequence and input and output files used are listed. The output files marked with a "*" are unique and have been saved. If not otherwise stated all files reside on /files/home/users/kemhl/0244. With regard to the permafrost calculations at the Finnsjön site, see Table of Contents below.

For further information with regard to file-name conventions and the contents on the files referred to in this Appendix, see "HYPAC User's Guide", B. Grundfelt, et al, Kemakta Report AR 89-18, Kemakta Consultants Co., Stockholm, Sweden, 1989.

Contents : **Page**

Pre-study (Regional) calculations

All cases (The mesh created was to big to be held in one file. The limit lies within the Finite Element generator FEMGEN. Hence, the mesh generation was split into two parts, part L defining the mesh to the left of the ice-edge, and part R defining the mesh to the right of the ice-edge.)

PreProcessing - Mesh Generation

PFG : (Before PFG was run EMC was run. No errors or duplicate nodes where found)

Input - Mesh	=	reg/pre/reg-l.neu *
Output - Mesh	=	reg/pre/reg-l.PFG
Output - Code	=	reg/pre/reg-l.PFC
Input - Mesh	=	reg/pre/reg-r.neu *
Output - Mesh	=	reg/pre/reg-r.PFG
Output - Code	=	reg/pre/reg-r.PFC

JTM : (The final mesh consisted of 7200 elements and 21989 nodes.)

Input - Mesh1	=	reg/pre/reg-l.PFG
Input - Code1	=	reg/pre/reg-l.PFC
Input - Mesh2	=	reg/pre/reg-r.PFG
Input - Code2	=	reg/pre/reg-r.PFC
Output - Mesh	=	reg/pre/reg.JTG
Output - Code	=	reg/pre/reg.JTC

OPT : (The front width was reduced to 106)

Input - Mesh	=	reg/pre/reg.JTG
Input - Code	=	reg/pre/reg.JTC
Output - Mesh	=	reg/pre/reg.OPG *
Output - Code	=	reg/pre/reg.OPC *

Case reg1

PreProcessing - Property assignment

BCA : (The topnodes from the left edge to the ice-edge was assigned a pressure value corresponding to the shape of the glacier.)

Input - Mesh	=	reg/pre/reg.OPG
Input - Code	=	reg/pre/reg.OPC
Input - Script	=	reg/bca/dobca *
Output - Mesh	=	reg/bca/reg.BCG

PEA : (All elements was assigned a hydraulic conductivity of $1.0 \cdot 10^{-6} \cdot z^{-1.1}$ m/s)

Input - Mesh	=	reg/bca/reg.BCG
Input - Code	=	reg/pre/reg.OPC
Output - Mesh	=	reg/pre/reg.PEG *

Nammu and PostProcessing

NAMMU :

Input - Mesh	=	reg/pre/reg.PEG
Input - Nammu	=	reg/nammu/reg.nam *
Output - Res	=	reg/nammu/reg.res *

TRG :

Input - Mesh	=	reg/pre/reg.PEG
Input - Code	=	reg/pre/reg.OPC
Input - Res	=	reg/nammu/reg.res

Vertical flux evaluation at 4 horizontal positions :

Input - Script	=	reg/post/dotrg1[a-d] *
Output - Flux	=	reg/post/reg.[1-4].DAT

Flux distribution at top-surface :

Input - Script	=	reg/post/dotrgft1 *
Output - Flux	=	reg/post/regft.DAT

Case reg1p

PreProcessing - Property assignment

PEA : (The area outlining the permafrost was assigned a hydraulic conductivity of $1.0 \cdot 10^{-16}$ m/s)

Input - Mesh	=	reg/pre/reg.PEG
Input - Code	=	reg/pre/reg.OPC
Input - Script	=	reg/pre/dopea1p *
Output - Mesh	=	reg/pre/reg1p.PEG *

Nammu and PostProcessing

NAMMU :

Input - Mesh	=	reg/pre/reg1p.PEG
Input - Nammu	=	reg/nammu/reg1p.nam *
Output - Res	=	reg/nammu/reg1p.res *

TRG :

Input - Mesh	=	reg/pre/reg1p.PEG
Input - Code	=	reg/pre/reg.OPC
Input - Res	=	reg/nammu/reg1p.res

Vertical flux evaluation at 4 horizontal positions :

Input - Script	=	reg/post/dotrg1p[a-d] *
Output - Flux	=	reg/post/reg1p[1-4].DAT

Case reg2

PreProcessing - Property assignment

BCA : (The topnodes from the left edge to the ice-edge was assigned a pressure value corresponding to average head of the ice-load = 1000 m.)

Input - Mesh	=	reg/pre/reg.OPG
Input - Code	=	reg/pre/reg.OPC
Input - Script	=	reg/bca/dobca2 *
Output - Mesh	=	reg/bca/reg2.BCG

PEA : (All elements was assigned a hydraulic conductivity of $1.0 \cdot 10^{-6} \cdot z^{-1.1}$ m/s)

Input - Mesh	=	reg/bca/reg2.BCG
Input - Code	=	reg/pre/reg.OPC
Output - Mesh	=	reg/pre/reg2.PEG *

Nammu and PostProcessing

NAMMU :

Input - Mesh	=	reg/pre/reg2.PEG
Input - Nammu	=	reg/nammu/reg2.nam *
Output - Res	=	reg/nammu/reg2.res *

TRG :

Input - Mesh	=	reg/pre/reg2.PEG
Input - Code	=	reg/pre/reg.OPC
Input - Res	=	reg/nammu/reg2.res

Vertical flux evaluation at 4 horizontal positions :

Input - Script	=	reg/post/dotrg2[a-d] *
Output - Flux	=	reg/post/reg[a-d].DAT

Case reg2p

PreProcessing - Property assignment

PEA : (The area outlining the permafrost was assigned a hydraulic conductivity of $1.0 \cdot 10^{-16}$ m/s)

Input - Mesh	=	reg/pre/reg2.PEG
Input - Code	=	reg/pre/reg.OPC
Input - Script	=	reg/pre/dopea2p *
Output - Mesh	=	reg/pre/reg2p.PEG *

Glaciation (Local) calculations

All cases (The mesh created was to big to be held in one file. The limit lies within the Finite Element generator FEMGEN. Hence, the mesh generation was split into three parts, part L defining the mesh to the left of the ice-edge, and part R1 defining the mesh from the ice-edge to the middle of the right part, and part R2 defining the rest of the mesh.)

PreProcessing - Mesh Generation

PFG : (Before PFG was run EMC was run. No errors or duplicate nodes where found)

Input - Mesh	=	loc/pre/loc-l.neu *
Output - Mesh	=	loc/pre/loc-l.PFG
Output - Code	=	loc/pre/loc-l.PFC
Input - Mesh	=	loc/pre/loc-r1.neu *
Output - Mesh	=	loc/pre/loc-r1.PFG
Output - Code	=	loc/pre/loc-r1.PFC
Input - Mesh	=	loc/pre/loc-r2.neu *
Output - Mesh	=	loc/pre/loc-r2.PFG
Output - Code	=	loc/pre/loc-r2.PFC

JTM : (The final mesh consisted of 9648 elements and 29367 nodes.)

Input - Script	=	loc/pre/dojtmlr1 *
Input - Mesh1	=	loc/pre/loc-l.PFG
Input - Code1	=	loc/pre/loc-l.PFC
Input - Mesh2	=	loc/pre/loc-r1.PFG
Input - Code2	=	loc/pre/loc-r1.PFC
Output - Mesh	=	loc/pre/loc-lr1.JTG
Output - Code	=	loc/pre/loclr1.JTC

Second join :

Input - Script	=	loc/pre/dojtmlr2 *
Input - Mesh1	=	loc/pre/loc-lr1.PFG
Input - Code1	=	loc/pre/loc-lr1.PFC
Input - Mesh2	=	loc/pre/loc-r2.PFG
Input - Code2	=	loc/pre/loc-r2.PFC
Output - Mesh	=	loc/pre/loc.JTG
Output - Code	=	loc/pre/loc.JTC

OPT : (The front width was reduced to 140)

Input - Mesh	=	loc/pre/loc.JTG
Input - Code	=	loc/pre/loc.JTC
Output - Mesh	=	loc/pre/loc.OPG *
Output - Code	=	loc/pre/loc.OPC *

Case loc1

PreProcessing - Property assignment

TBC : (Transfering of pressure from the regional model reg1.)

Input - MeshR	=	reg/pre/reg.PEG
Input - ResR	=	reg/nammu/reg.res
Input - MeshL	=	loc/pre/loc.OPG
Input - Script	=	loc/pre2/dotbc1 *
Output - Mesh	=	loc/pre2/loc.TBG

BCA : (The topnodes from the left edge to the ice-edge was assigned a pressure value corresponding to the shape of the glacier. The right lateral boundary was assigned as No-Flow.)

Input - Mesh	=	loc/pre2/loc.TBG
Input - Code	=	loc/pre/loc.OPC
Input - Script	=	loc/pre2/dobca1 *
Output - Mesh	=	loc/pre2/loc.BCG

PEA : (All elements was assigned a hydraulic conductivity of $1.0 \cdot 10^{-6} \cdot z^{-1.1}$ m/s)

Input - Mesh	=	loc/pre2/loc.BCG
Input - Code	=	loc/pre/loc.OPC
Input - Script	=	loc/pre2/dopea1 *
Output - Mesh	=	loc/pre2/loc1.PEG *

Nammu and PostProcessing

NAMMU :

Input - Mesh	=	loc/pre2/loc1.PEG
Input - Nammu	=	loc/nammu/loc1.nam *
Output - Res	=	loc/nammu/loc1.res *

TRG :

Input - Mesh	=	loc/pre2/loc1.PEG
Input - Code	=	loc/pre/loc.OPC
Input - Res	=	loc/nammu/loc1.res

Flux along line at repository level :

Input - Script	=	loc/post/dotrgf1 *
Output - Flux	=	loc/post/loc1f.DAT

Flux distribution at top-surface :

Input - Script	=	loc/post/dotrgft1 *
Output - Flux	=	loc/post/loc1ft.DAT

Pathlines :

Input - Script	=	loc/post/doban1 *
Output - Paths	=	loc/post/loc1bB[1-8].DAT

Travel times along line at repository level :
Input - Script = loc/post/dobanm1 *
Output - Times = loc/post/loc1bm.LBN

Case loc1p

PreProcessing - Property assignment

PEA : (The area outlining the permafrost was assigned a hydraulic conductivity of $1.0 \cdot 10^{-16}$ m/s)

Input - Mesh = loc/pre2/loc1.PEG
Input - Code = loc/pre/loc.OPC
Input - Script = loc/pre2/dopea1p *
Output - Mesh = loc/pre2/loc1p.PEG *

Nammu and PostProcessing

NAMMU :

Input - Mesh = loc/pre2/loc1p.PEG
Input - Nammu = loc/nammu/loc1p.nam *
Output - Res = loc/nammu/loc1p.res *

TRG :

Input - Mesh = loc/pre2/loc1p.PEG
Input - Code = loc/pre/loc.OPC
Input - Res = loc/nammu/loc1p.res

Flux along line at repository level :
Input - Script = loc/post/dotrgf1p *
Output - Flux = loc/post/loc1pf.DAT

Flux distribution at top-surface :
Input - Script = loc/post/dotrgft1p *
Output - Flux = loc/post/loc1pft.DAT

Pathlines :
Input - Script = loc/post/doban1p *
Output - Paths = loc/post/loc1pbB[1-8].DAT

Travel times along line at repository level :
Input - Script = loc/post/dobanm1p *
Output - Times = loc/post/loc1pbm.LBN

Case loc2

PreProcessing - Property assignment

TBC : (Transfering of pressure from the regional model reg2.)

Input - MeshR	=	reg/pre/reg2.PEG
Input - ResR	=	reg/nammu/reg2.res
Input - MeshL	=	loc/pre/loc.OPG
Input - Script	=	loc/pre2/dotbc2 *
Output - Mesh	=	loc/pre2/loc2.TBG

BCA : (The topnodes from the left edge to the ice-edge was assigned a pressure value corresponding to the average head of the glacier = 1000 m.)

Input - Mesh	=	loc/pre2/loc2.TBG
Input - Code	=	loc/pre/loc.OPC
Input - Script	=	loc/pre2/dobca2 *
Output - Mesh	=	loc/pre2/loc2.BCG

PEA : (All elements was assigned a hydraulic conductivity of $1.0 \cdot 10^{-6} \cdot z^{-1.1}$ m/s)

Input - Mesh	=	loc/pre2/loc2.BCG
Input - Code	=	loc/pre/loc.OPC
Input - Script	=	loc/pre2/dopea2 *
Output - Mesh	=	loc/pre2/loc2.PEG *

Nammu and PostProcessing

NAMMU :

Input - Mesh	=	loc/pre2/loc2.PEG
Input - Nammu	=	loc/nammu/loc2.nam *
Output - Res	=	loc/nammu/loc2.res *

TRG :

Input - Mesh	=	loc/pre2/loc2.PEG
Input - Code	=	loc/pre/loc.OPC
Input - Res	=	loc/nammu/loc2.res

Flux along line at repository level :

Input - Script	=	loc/post2/dotrgf2 *
Output - Flux	=	loc/post2/loc2f.DAT

Pathlines :

Input - Script	=	loc/post2/doban2 *
Output - Paths	=	loc/post2/loc2bB[1-8].DAT

Travel times along line at repository level :

Input - Script	=	loc/post2/dobanm2 *
Output - Times	=	loc/post2/loc2bm.LBN

Case loc2p

PreProcessing - Property assignment

TBC : (Transfering of pressure from the regional model reg2p.)

Input - MeshR	=	reg/pre/reg2p.PEG
Input - ResR	=	reg/nammu/reg2p.res
Input - MeshL	=	loc/pre/loc.OPG
Input - Script	=	loc/pre2/dotbc2p *
Output - Mesh	=	loc/pre2/loc2p.TBG

BCA : (The topnodes from the left edge to the ice-edge was assigned a pressure value corresponding to the average head of the glacier = 1000 m.)

Input - Mesh	=	loc/pre2/loc2p.TBG
Input - Code	=	loc/pre/loc.OPC
Input - Script	=	loc/pre2/dobca2p *
Output - Mesh	=	loc/pre2/loc2p.BCG

PEA : (All elements was assigned a hydraulic conductivity of $1.0 \cdot 10^{-6} \cdot z^{-1.1}$ m/s. The area outlining the permafrost was assigned a hydraulic conductivity of $1.0 \cdot 10^{-16}$ m/s.)

Input - Mesh	=	loc/pre2/loc2p.BCG
Input - Code	=	loc/pre/loc.OPC
Input - Script	=	loc/pre2/dopea2p *
Output - Mesh	=	loc/pre2/loc2p.PEG *

Nammu and PostProcessing

NAMMU :

Input - Mesh	=	loc/pre2/loc2p.PEG
Input - Nammu	=	loc/nammu/loc2p.nam *
Output - Res	=	loc/nammu/loc2p.res *

TRG :

Input - Mesh	=	loc/pre2/loc2p.PEG
Input - Code	=	loc/pre/loc.OPC
Input - Res	=	loc/nammu/loc2p.res

Flux along line at repository level :

Input - Script	=	loc/post2/dotrgf2p *
Output - Flux	=	loc/post2/loc2pf.DAT

Pathlines :

Input - Script	=	loc/post2/doban2p *
Output - Paths	=	loc/post2/loc2pbB[1-8].DAT

Travel times along line at repository level :

Input - Script	=	loc/post2/dobanm2p *
Output - Times	=	loc/post2/loc2pbm.LBN

For each case the program sequence and input and output files used are listed. The output files marked with a "*" are unique and have been saved. If not otherwise stated all files reside on /files/home/users/kemhl/0243.

For further information with regard to file-name conventions and the contents on the files referred to in this Appendix, see "HYPAC User's Guide", B. Grundfelt, et al, Kemakta Report AR 89-18, Kemakta Consultants Co., Stockholm, Sweden, 1989.

Two new utility HYPAC programs have been developed for this project : **GetPath** reads the pathline output file (*.BAN) generated by TRG and 1) Splits the individual files into separate files named <*casename*>BANB*X*.DAT where *X* is the pathline number, and 2) generates a file called <*casename*>.LBN holding the total accumulated travel time and length for each pathline. **Convrt** reads either a GRD-file generated for Topo by TRG or the output from FPR and converts the flux-values from [$m^3/m^2/s$] to [$ml/m^2/year$].

Contents

2D Permafrost calculations

PreProcessing

PFG :

Input - Mesh	=	perm/pre/fin2dp.neu *
Output - Mesh	=	perm/pre/fin2dp.PFG *
Output - Code	=	perm/pre/fin2dp.PFC *

OPT :

Input - Mesh	=	perm/pre/fin2dp.PFG
Input - Code	=	perm/pre/fin2dp.PFC
Output - Mesh	=	perm/pre/fin2dp.OPG *
Output - Code	=	perm/pre/fin2dp.OPC *

BCA :

Input - Mesh	=	perm/pre/fin2dp.OPG
Input - Code	=	perm/pre/fin2dp.OPC
Input - Script	=	perm/pre/dobca *
Output - Mesh	=	perm/pre/fin2dp.BCG *

Nammu and PostProcessing for the four cases

CASE pf1 (No permafrost)

PEA :

Input - Mesh	=	perm/pre/fin2dp.BCG
Input - Code	=	perm/pre/fin2dp.OPC
Input - Script	=	perm/pre/dopeapf1 *
Output - Mesh	=	perm/pre/fin2dpf1.PEG *

NAMMU :

Input - Mesh	=	perm/pre/fin2dpf1.PEG
Input - Nammu	=	perm/nammu/pf1.nam *
Output - Res	=	perm/nammu/pf1.res *

TRG :

Input - Mesh	=	perm/pre/fin2dpf1.PEG
Input - Code	=	perm/pre/fin2dp.OPC
Input - Res	=	perm/nammu/pf1.res

Pathlines :
The program (hypac) getpath is used to generate the Pathstat file and the separate pathline files.

Input - Script = perm/trg/dobanpf1 *
Output - Paths = perm/trg/pf1ban.BAN
Output - PathStat = perm/trg/pf1ban.LBN

Isoflux :
Input - Script = perm/trg/dotrgpf1 *
Output - Flux = perm/trg/pf1.FLX
Output - Topo = perm/trg/pf1.GRD
OutputConvTopo = perm/trg/pf1c.GRD

CASE pf2 (Permafrost down to a level between zone 2 and the ground surface)

PEA :

Input - Mesh = perm/pre/fin2dp.BCG
Input - Code = perm/pre/fin2dp.OPC
Input - Script = perm/pea/dopeapf2 *
Output - Mesh = perm/pea/fin2dpf2.PEG *

NAMMU :

Input - Mesh = perm/pea/fin2dpf2.PEG
Input - Nammu = perm/nammu/pf2.nam *
Output - Res = perm/nammu/pf2.res *

TRG :

Input - Mesh = perm/pea/fin2dpf2.PEG
Input - Code = perm/pre/fin2dp.OPC
Input - Res = perm/nammu/pf2.res

Pathlines :
The program (hypac) getpath is used to generate the Pathstat file and the separate pathline files.

Input - Script = perm/trg/dobanpf2 *
Output - Paths = perm/trg/pf2ban.BAN
Output - PathStat = perm/trg/pf2ban.LBN

Isoflux :
Input - Script = perm/trg/dotrgpf2 *
Output - Flux = perm/trg/pf2.FLX
Output - Topo = perm/trg/pf2.GRD
OutputConvTopo = perm/trg/pf2c.GRD

CASE pf3 (Permafrost down to the lower limit of zone 2)

PEA :

Input - Mesh = perm/pre/fin2dp.BCG
Input - Code = perm/pre/fin2dp.OPC
Input - Script = perm/pea/dopeapf3 *
Output - Mesh = perm/pea/fin2dpf3.PEG *

NAMMU :

Input - Mesh	=	perm/pea/fin2dpf3.PEG
Input - Nammu	=	perm/nammu/pf3.nam *
Output - Res	=	perm/nammu/pf3.res *

TRG :

Input - Mesh	=	perm/pea/fin2dpf3.PEG
Input - Code	=	perm/pre/fin2dp.OPC
Input - Res	=	perm/nammu/pf3.res

Pathlines :
The program (hypac) getpath is used to generate the Pathstat file and the separate pathline files.

Input - Script	=	perm/trg/dobanpf3 *
Output - Paths	=	perm/trg/pf3banB[1..8].BAN
Output - PathStat	=	perm/trg/pf3ban.LBN

Isoflux :

Input - Script	=	perm/trg/dotrgpf3 *
Output - Flux	=	perm/trg/pf3.FLX
Output - Topo	=	perm/trg/pf3.GRD
OutputConvTopo	=	perm/trg/pf3c.GRD

CASE pf4 (Permafrost down to -700 m)

PEA :

Input - Mesh	=	perm/pre/fin2dp.BCG
Input - Code	=	perm/pre/fin2dp.OPC
Input - Script	=	perm/pea/dopeapf4 *
Output - Mesh	=	perm/pea/fin2dpf4.PEG *

NAMMU :

Input - Mesh	=	perm/pea/fin2dpf4.PEG
Input - Nammu	=	perm/nammu/pf4.nam *
Output - Res	=	perm/nammu/pf4.res *

TRG :

Input - Mesh	=	perm/pea/fin2dpf4.PEG
Input - Code	=	perm/pre/fin2dp.OPC
Input - Res	=	perm/nammu/pf4.res

Pathlines :
The program (hypac) getpath is used to generate the Pathstat file and the separate pathline files.

Input - Script	=	perm/trg/dobanpf4 *
Output - Paths	=	perm/trg/pf4banB[1..8].BAN
Output - PathStat	=	perm/trg/pf4ban.LBN

Isoflux :

Input - Script	=	perm/trg/dotrgpf4 *
Output - Flux	=	perm/trg/pf4.FLX
Output - Topo	=	perm/trg/pf4.GRD
OutputConvTopo	=	perm/trg/pf4c.GRD

List of SKB reports

Annual Reports

1977-78
TR 121
KBS Technical Reports 1 – 120
Summaries
Stockholm, May 1979

1979
TR 79-28
The KBS Annual Report 1979
KBS Technical Reports 79-01 – 79-27
Summaries
Stockholm, March 1980

1980
TR 80-26
The KBS Annual Report 1980
KBS Technical Reports 80-01 – 80-25
Summaries
Stockholm, March 1981

1981
TR 81-17
The KBS Annual Report 1981
KBS Technical Reports 81-01 – 81-16
Summaries
Stockholm, April 1982

1982
TR 82-28
The KBS Annual Report 1982
KBS Technical Reports 82-01 – 82-27
Summaries
Stockholm, July 1983

1983
TR 83-77
The KBS Annual Report 1983
KBS Technical Reports 83-01 – 83-76
Summaries
Stockholm, June 1984

1984
TR 85-01
Annual Research and Development Report 1984
Including Summaries of Technical Reports Issued during 1984. (Technical Reports 84-01 – 84-19)
Stockholm, June 1985

1985
TR 85-20
Annual Research and Development Report 1985
Including Summaries of Technical Reports Issued during 1985. (Technical Reports 85-01 – 85-19)
Stockholm, May 1986

1986
TR 86-31
SKB Annual Report 1986
Including Summaries of Technical Reports Issued during 1986
Stockholm, May 1987

1987
TR 87-33
SKB Annual Report 1987
Including Summaries of Technical Reports Issued during 1987
Stockholm, May 1988

1988
TR 88-32
SKB Annual Report 1988
Including Summaries of Technical Reports Issued during 1988
Stockholm, May 1989

1989
TR 89-40
SKB Annual Report 1989
Including Summaries of Technical Reports Issued during 1989
Stockholm, May 1990

1990
TR 90-46
SKB Annual Report 1990
Including Summaries of Technical Reports Issued during 1990
Stockholm, May 1991

Technical Reports

List of SKB Technical Reports 1991

TR 91-01
Description of geological data in SKB's database GEOTAB
Version 2
Stefan Sehlstedt, Tomas Stark
SGAB, Luleå
January 1991

TR 91-02
Description of geophysical data in SKB database GEOTAB
Version 2
Stefan Sehlstedt
SGAB, Luleå
January 1991

TR 91-03
1. The application of PIE techniques to the study of the corrosion of spent oxide fuel in deep-rock ground waters
2. Spent fuel degradation
R S Forsyth
Studsvik Nuclear
January 1991

TR 91-04
Plutonium solubilities
I Puigdomènech[1], J Bruno[2]
[1]Enviromental Services, Studsvik Nuclear, Nyköping, Sweden
[2]MBT Tecnologia Ambiental, CENT, Cerdanyola, Spain
February 1991

TR 91-05
Description of tracer data in the SKB database GEOTAB
SGAB, Luleå
April, 1991

TR 91-06
Description of background data in the SKB database GEOTAB
Version 2
Ebbe Eriksson, Stefan Sehlstedt
SGAB, Luleå
March 1991

TR 91-07
Description of hydrogeological data in the SKB's database GEOTAB
Version 2
Margareta Gerlach (ed.)
Mark Radon Miljö MRM Konsult AB, Luleå
December 1991

TR 91-08
Overview of geologic and geohydrologic conditions at the Finnsjön site and its surroundings
Kaj Ahlbom[1], Sven Tirén[2]
[1]Conterra AB
[2]Sveriges Geologiska AB
January 1991

TR 91-09
Long term sampling and measuring program. Joint report for 1987, 1988 and 1989. Within the project: Fallout studies in the Gideå and Finnsjö areas after the Chernobyl accident in 1986
Thomas Ittner
SGAB, Uppsala
December 1990

TR 91-10
Sealing of rock joints by induced calcite precipitation. A case study from Bergeforsen hydro power plant
Eva Hakami[1], Anders Ekstav[2], Ulf Qvarfort[2]
[1]Vattenfall HydroPower AB
[2]Golder Geosystem AB
January 1991

TR 91-11
Impact from the disturbed zone on nuclide migration – a radioactive waste repository study
Akke Bengtsson[1], Bertil Grundfelt[1], Anders Markström[1], Anders Rasmuson[2]
[1]KEMAKTA Konsult AB
[2]Chalmers Institute of Technology
January 1991

TR 91-12
Numerical groundwater flow calculations at the Finnsjön site
Björn Lindbom, Anders Boghammar, Hans Lindberg, Jan Bjelkås
KEMAKTA Consultants Co, Stockholm
February 1991

TR 91-13
Discrete fracture modelling of the Finnsjön rock mass
Phase 1 feasibility study
J E Geier, C-L Axelsson
Golder Geosystem AB, Uppsala
March 1991

TR 91-14
Channel widths
Kai Palmqvist, Marianne Lindström
BERGAB-Berggeologiska Undersökningar AB
February 1991

TR 91-15
Uraninite alteration in an oxidizing environment and its relevance to the disposal of spent nuclear fuel
Robert Finch, Rodney Ewing
Department of Geology, University of New Mexico
December 1990

TR 91-16
Porosity, sorption and diffusivity data compiled for the SKB 91 study
Fredrik Brandberg, Kristina Skagius
Kemakta Consultants Co, Stockholm
April 1991

TR 91-17
Seismically deformed sediments in the Lansjärv area, Northern Sweden
Robert Lagerbäck
May 1991

TR 91-18
Numerical inversion of Laplace transforms using integration and convergence acceleration
Sven-Åke Gustafson
Rogaland University, Stavanger, Norway
May 1991

TR 91-19
NEAR21 - A near field radionuclide migration code for use with the PROPER package
Sven Norman[1], Nils Kjellbert[2]
[1]Starprog AB
[2]SKB AB
April 1991

TR 91-20
Äspö Hard Rock Laboratory. Overview of the investigations 1986-1990
R Stanfors, M Erlström, I Markström
June 1991

TR 91-21
Äspö Hard Rock Laboratory. Field investigation methodology and instruments used in the pre-investigation phase, 1986-1990
K-E Almén, O Zellman
June 1991

TR 91-22
Äspö Hard Rock Laboratory. Evaluation and conceptual modelling based on the pre-investigations 1986-1990
P Wikberg, G Gustafson, I Rhén, R Stanfors
June 1991

TR 91-23
Äspö Hard Rock Laboratory. Predictions prior to excavation and the process of their validation
Gunnar Gustafson, Magnus Liedholm, Ingvar Rhén, Roy Stanfors, Peter Wikberg
June 1991

TR 91-24
Hydrogeological conditions in the Finnsjön area. Compilation of data and conceptual model
Jan-Erik Andersson, Rune Nordqvist, Göran Nyberg, John Smellie, Sven Tirén
February 1991

TR 91-25
The role of the disturbed rock zone in radioactive waste repository safety and performance assessment. A topical discussion and international overview.
Anders Winberg
June 1991

TR 91-26
Testing of parameter averaging techniques for far-field migration calculations using FARF31 with varying velocity.
Akke Bengtsson[1], Anders Boghammar[1], Bertil Grundfelt[1], Anders Rasmuson[2]
[1]KEMAKTA Consultants Co
[2]Chalmers Institute of Technology

TR 91-27
Verification of HYDRASTAR. A code for stochastic continuum simulation of groundwater flow
Sven Norman
Starprog AB
July 1991

TR 91-28
Radionuclide content in surface and groundwater transformed into breakthrough curves. A Chernobyl fallout study in an forested area in Northern Sweden
Thomas Ittner, Erik Gustafsson, Rune Nordqvist
SGAB, Uppsala
June 1991

TR 91-29
Soil map, area and volume calculations in Orrmyrberget catchment basin at Gideå, Northern Sweden
Thomas Ittner, P-T Tammela, Erik Gustafsson
SGAB, Uppsala
June 1991

TR 91-30
A resistance network model for radionuclide transport into the near field surrounding a repository for nuclear waste (SKB, Near Field Model 91)
Lennart Nilsson, Luis Moreno, Ivars Neretnieks, Leonardo Romero
Department of Chemical Engineering,
Royal Institute of Technology, Stockholm
June 1991

TR 91-31
Near field studies within the SKB 91 project
Hans Widén, Akke Bengtsson, Bertil Grundfelt
Kemakta Consultants AB, Stockholm
June 1991

TR 91-32
SKB/TVO Ice age scenario
Kaj Ahlbom[1], Timo Äikäs[2], Lars O. Ericsson[3]
[1]Conterra AB
[2]Teollisuuden Voima Oy (TVO)
[3]Svensk Kärnbränslehantering AB (SKB)
June 1991

TR 91-33
Transient nuclide release through the bentonite barrier - SKB 91
Akke Bengtsson, Hans Widén
Kemakta Konsult AB
May 1991

TR 91-34
SIMFUEL dissolution studies in granitic groundwater
I Casas[1], A Sandino[2], M S Caceci[1], J Bruno[1], K Ollila[3]
[1]MBT Tecnologia Ambiental, CENT, Cerdanyola, Spain
[2]KTH, Dpt. of Inorganic Chemistry, Stockholm, Sweden
[3]VTT, Tech. Res. Center of Finland, Espoo, Finland
September 1991

TR 91-35
Storage of nuclear waste in long boreholes
Håkan Sandstedt[1], Curt Wichmann[1], Roland Pusch[2], Lennart Börgesson[2], Bengt Lönnerberg[3]
[1]Tyréns
[2]Clay Technology AB
[3]ABB Atom
August 1991

TR 91-36
Tentative outline and siting of a repository for spent nuclear fuel at the Finnsjön site. SKB 91 reference concept
Lars Ageskog, Kjell Sjödin
VBB VIAK
September 1991

TR 91-37
Creep of OFHC and silver copper at simulated final repository canister-service conditions
Pertti Auerkari, Heikki Leinonen, Stefan Sandlin
VTT, Metals Laboratory, Finland
September 1991

TR 91-38
Production methods and costs of oxygen free copper canisters for nuclear waste disposal
Hannu Rajainmäki, Mikko Nieminen, Lenni Laakso
Outokumpu Poricopper Oy, Finland
June 1991

TR 91-39
The reducibility of sulphuric acid and sulphate in aqueous solution (translated from German)
Rolf Grauer
Paul Scherrer Institute, Switzerland
July 1990

TR 91-40
Interaction between geosphere and biosphere in lake sediments
Björn Sundblad, Ignasi Puigdomenech, Lena Mathiasson
December 1990

TR 91-41
Individual doses from radionuclides released to the Baltic coast
Ulla Bergström, Sture Nordlinder
Studsvik AB
May 1991

TR 91-42
Sensitivity analysis of the groundwater flow at the Finnsjön study site
Yung-Bing Bao, Roger Thunvik
Dept. Land and Water Resources,
Royal Institute of Technology, Stockholm, Sweden
September 1991

TR 91-43
SKB - PNC
Development of tunnel radar antennas
Lars Falk
ABEM, Uppsala, Sweden
July 1991

TR 91-44
Fluid and solute transport in a network of channels
Luis Moreno, Ivars Neretnieks
Department of Chemical Engineering,
Royal Institute of Technology, Stockholm, Sweden
September 1991

TR 91-45
The implications of soil acidification on a future HLNW repository.
Part I: The effects of increased weathering, erosion and deforestation
Josefa Nebot, Jordi Bruno
MBT Tecnologìa Ambiental, Cerdanyola, Spain
July 1991

TR 91-46
Some mechanisms which may reduce radiolysis
Ivars Neretnieks, Mostapha Faghihi
Department of Chemical Engineering, Royal Institute of Technology, Stockholm, Sweden
August 1991

TR 91-47
On the interaction of granite with Tc(IV) and Tc(VII) in aqueous solution
Trygve E Eriksen, Daquing Cui
Royal Institute of Technology, Department of Nuclear Chemistry, Stockholm, Sweden
October 1991

TR 91-48
A compartment model for solute transport in the near field of a respository for radioactive waste (Calculations for Pu-239)
Leonardo Romero, Luis Moreno , Ivars Neretnieks
Department of Chemical Engineering, Royal Institute of Technology, Stockholm, Sweden
October 1991

TR 91-49
Description of transport pathways in a KBS-3 type repository
Roland Pusch[1], Ivars Neretnieks[2], Patrik Sellin[3]
[1] Clay Technology AB. Lund
[2] The Royal institue of Techonology Department of Chemical Engineering, Stockholm
[3] Swedisch Nueclear Fuel and Waste Management Co (SKB), Stockholm
December 1991

TR 91-50
Concentrations of particulate matter and humic substances in deep groundwaters and estimated effects on the adsorption and transport of radionuclides
Bert Allard[1], Fred Karlsson[2], Ivars Neretnieks[3]
[1]Department of Water and Environmental Studies, University of Linköping, Sweden
[2]Swedish Nuclear Fuel and Waste Management Company, SKB, Stockholm, Sweden
[3]Department of Chemical Engineering, Royal Institute of Technology, Stockholm, Sweden
November 1991

TR 91-51
Gideå study site. Scope of activities and main results
Kaj Ahlbom[1], Jan-Erik Andersson[2],
Rune Nordqvist[2], Christer Ljunggren[2], Sven Tirén[2],
Clifford Voss[3]
[1]Conterra AB
[2]Geosigma AB
[3]U.S. Geological Survey
October 1991

TR 91-52
Fjällveden study site. Scope of activities and main results
Kaj Ahlbom[1], Jan-Erik Andersson[2],
Rune Nordqvist[2], Christer Ljunggren[2], Sven Tirén[2],
Clifford Voss[3]
[1]Conterra AB
[2]Geosigma AB
[3]U.S. Geological Survey
October 1991

TR 91-53
Impact of a repository on permafrost development during glaciation advance
Per Vallander, Jan Eurenius
VBB VIAK AB
December 1991

TR 91-54

Hydraulic evaluation of the groundwater conditions at Finnsjön. The effects on dilution in a domestic well

C-L Axelsson[1], J Byström[1], Å Eriksson[1],
J Holmén[1], H M Haitjema[2]
[1]Golder Geosystem AB, Uppsala, Sweden
[2]School of Public and Environmental Affairs,
Indiana University, Bloomington, Indiana, USA
September 1991

TR 91-55

Redox capacity of crystalline rocks. Laboratory studies under 100 bar oxygen gas pressure

Veijo Pirhonen, Petteri Pitkänen
Technical Research Center of Finland
December 1991

TR 91-56

Microbes in crystalline bedrock. Assimilation of CO_2 and introduced organic compounds by bacterial populations in groundwater from deep crystalline bedrock at Laxemar and Stripa

Karsten Pedersen, Susanne Ekendahl,
Johanna Arlinger
Department of General and Marine Microbiology,
University of Göteborg, Göteborg, Sweden
December 1991

TR 91-57

The groundwater circulation in the Finnsjö area - the impact of density gradients

Part A: Saline groundwater at the Finnsjö site and its surroundings

Kaj Ahlbom
CONTERRA AB

Part B: A numerical study of the combined effects of salinity gradients, temperature gradients and fracture zones

Urban Svensson
CFE AB

Part C: A three-dimensional numerical model of groundwater flow and salinity distribution in the Finnsjö area

Urban Svensson
CFE AB
November 1991